Journal of Building Engineering 129 (2026) 116799

Contents lists available at ScienceDirect

Journal of Building Engineering

journal homepage: www.elsevier.com/locate/jobe

Experimental investigations and analytical models on Composite Reinforced Mortar (CRM) systems for masonry strengthening: a state-of-the-art review

Stefano De Santis [a,*], Maria Antonietta Aiello [b], Ingrid Boem [c], Silvia Calò [b], Alessio Cascardi [b,d], Tommaso D'Antino [e], Marielisa Di Leto [f], Natalino Gattesco [c], Lidia La Mendola [f], Francesco Micelli [b], Emanuele Rizzi [c], Emanuela Speranzini [g]

[a] Roma Tre University, Department of Civil, Computer and Aeronautical Engineering, Via Vito Volterra 62, Rome, 00146, Italy
[b] University of Salento, Department of Innovation Engineering, Via per Monteroni, Lecce, 73100, Italy
[c] University of Trieste, Department of Engineering and Architecture, Via Alfonso Valerio 6/1, Trieste, 34127, Italy
[d] University of Calabria, Department of Civil Engineering, Ponte Pietro Bucci, Arcavacata di Rende, CS, 87036, Italy
[e] Politecnico di Milano, Department of Architecture, Civil Engineering and Built Environment, Piazza Leonardo da Vinci 32, Milano, 20133, Italy
[f] University of Palermo, Department of Engineering, Viale delle Scienze, Palermo, 90128, Italy
[g] University of Perugia, Department of Engineering, Via Duranti 93, Perugia, 06125, Italy

ARTICLE INFO

Keywords:
Flexural strengthening
Shear strengthening
Mortar-based composites
Glass fibre reinforced polymer mesh
Experimental database

ABSTRACT

Composite Reinforced Mortar (CRM) is an emerging technique for strengthening masonry structures, based on the use of a pre-cured FRP mesh embedded within an inorganic matrix. Although CRM systems can be certified within the European Union, specific design codes are still lacking, and the available guidance remains fragmented. This paper provides an overview of experimental investigations carried out on CRM constituent materials to test mechanical properties and durability, and on structural members strengthened with CRM, such as masonry walls subjected to in-plane and out-of-plane actions, vaulted elements, and crowning beams. Existing analytical models for predicting the capacity of masonry elements retrofitted with CRM are reviewed and critically discussed in the light of experimental evidence. The shake table tests conducted to investigate the seismic behaviour of masonry structures strengthened with CRM are also described. Furthermore, the potential use of CRM for integrated energy-structural retrofitting solutions is examined, together with low-impact strategies suitable for fair-faced masonry applications and architectural heritage.

* Corresponding author.
E-mail addresses: stefano.desantis@uniroma3.it (S. De Santis), antonietta.aiello@unisalento.it (M.A. Aiello), ingrid.boem@dia.units.it (I. Boem), silvia.calo@unisalento.it (S. Calò), alessio.cascardi@unical.it (A. Cascardi), tommaso.dantino@polimi.it (T. D'Antino), marielisa.dileto@unipa.it (M. Di Leto), gattesco@units.it (N. Gattesco), lidia.lamendola@unipa.it (L. La Mendola), francesco.micelli@unisalento.it (F. Micelli), emanuele.rizzi@units.it (E. Rizzi), emanuela.speranzini@unipg.it (E. Speranzini).

https://doi.org/10.1016/j.jobe.2026.116799
Received 8 April 2026; Received in revised form 3 June 2026; Accepted 4 July 2026
Available online 8 July 2026
2352-7102/© 2026 The Authors. Published by Elsevier Ltd. This is an open access article under the CC BY license (http://creativecommons.org/licenses/by/4.0/).

1. Introduction

Composite Reinforced Mortar (CRM) is an innovative technology for strengthening masonry structures. It comprises an industrially prefabricated pre-cured mesh made from Fibre Reinforced Polymer (FRP) materials, such as AR glass, carbon, or basalt fibres, immersed in a thermosetting resin (Fig. 1a). The mesh is embedded within a mortar matrix, typically based on lime, cement, or geopolymer binders. The load transfer from the masonry to the mesh relies on two concurrent mechanisms. The first depends on the chemical bond between the matrix and the surface of the substrate and of the mesh and is ensured by the composite action developed within the hardened mortar layer, which provides adhesion, friction, and confinement around the fibres. The second is due to the mechanical connectors, made of either the same FRP material or steel, which are inserted into drilled holes and grouted with fast-curing thermosetting resins or mortars to guarantee a reliable anchorage to the substrate and to prevent premature debonding (especially out-of-plane). In some cases, an additional mesh patch is applied around the connector area to improve local stress distribution and enhance the overall transfer mechanism (Fig. 1b). The application procedure resembles that of traditional steel-reinforced plaster and can be performed either manually or by mechanical spraying (Fig. 1c). Nonetheless, because the reinforcement is not susceptible to galvanic corrosion, no minimum cover thickness is required beyond that needed to fully encapsulate the mesh and promote uniform stress transfer. However, the alkaline environment provided by the mortar matrix can still induce a slow, long-term degradation of the fibres, depending on their nature and protective coatings. For this reason, CRM systems are considered highly durable but not immune to ageing phenomena, and the mortar cover should be proportioned to ensure both adequate mechanical performance and long-term stability. Due to its mechanical characteristics and construction-related features, CRM is particularly suited to applications in masonry, which is characterized by relatively low stiffness (compared with reinforced concrete), negligible tensile strength, and rough surfaces. The high strength of CRM enhances the mechanical performance of strengthened masonry elements, effectively absorbing tensile stresses and thus increasing the masonry strength. Beyond these well-documented benefits, CRM systems can foster stress redistribution in the cracked stage, with potential benefits also in terms of deformation capacity and energy dissipation under seismic loading. Notable benefits can also arise from the constraints that prevent disaggregation and leaf separation, which are the most critical failure modes of rubblestone masonry built with multiple leaves, weak mortars, small units, and exhibiting poor connections at corners and with horizontal elements. Additionally, CRM exhibits good resistance to high temperatures, chemical-physical compatibility with masonry substrates, and, depending on the mortar used, vapor permeability. Lastly, it can be easily applied using traditional methods, even on damp, wet, and irregular surfaces.

These features, as discussed in the following sections, have been progressively evidenced by the research conducted primarily within the scientific community involved in the structural rehabilitation with composite materials, including FRP [1–5], and Fabric Reinforced Cementitious Matrix (FRCM) or Textile Reinforced Mortar (TRM) [6–13]. While FRP and FRCM/TRM are generally regarded as established externally bonded strengthening techniques, CRM systems are increasingly emerging as a reliable and effective alternative for a broad range of applications to masonry structures.

This progress is already being transferred into engineering practice through the development of product qualification procedures. CRM systems can now be certified within the European Union through the European Technical Assessment (ETA) [14], a step toward CE marking. In Italy, certification guidelines [15] lead to a Technical Assessment Certificate (CVT). On the other hand, there are currently no established design guidelines specifically developed for CRM systems. Amplification coefficients can be applied to the mechanical properties of masonry, as specified in the Italian Building Code [16] for traditional steel-reinforced plasters, a highly simplified approach to conduct global analyses. But it lacks specific validation for CRM and cannot be used for the assessment of local collapse mechanisms.

Alternatively, design methods developed for FRCM/TRM systems [17,18] can be adapted, though these mortar-based composites, while related, differ significantly from CRM. First, compared to FRCM/TRM, CRM includes meshes with larger spacing (30-100 mm versus 8-25 mm) and higher stiffness (precured FRP mesh instead of a dry, coated, or lightly pre-impregnated textile). Second, matrix

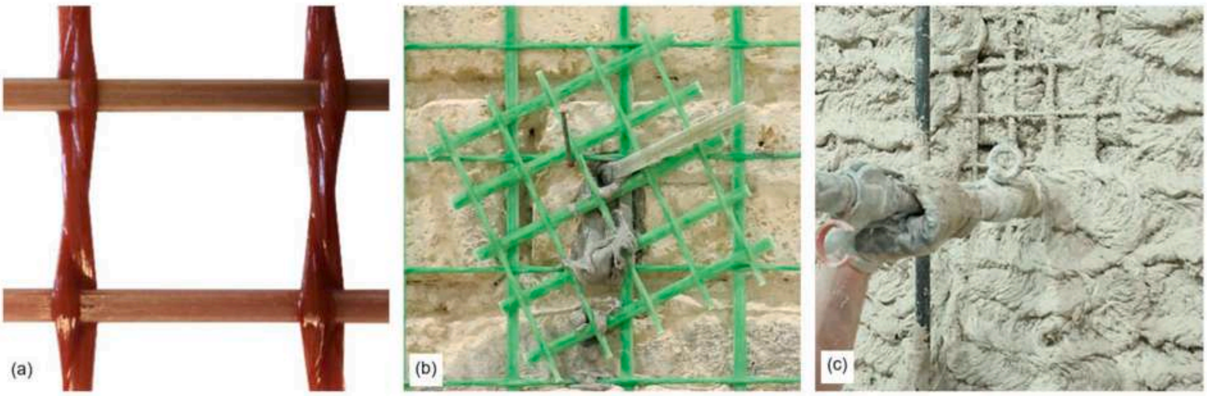

Fig. 1. FRP mesh of a CRM system (a); L-shaped FRP connector installed with an additional mesh patch (b); sprayed application of the mortar matrix (c).

layers are thicker (30-50 mm versus 8-12 mm). Third, the presence of mechanical connections is essential and CRM systems always include them according to existing qualification codes, while provisions dealing with FRCM/TRM do not mandate the use of connectors. Finally, certification is conducted according to different mechanical characterization protocols, since CRM mesh and mortar are certified separately and the mesh is tested under tensile loading only, while FRCM/TRM are qualified as a composite and shear bond tests are essential. These features highlight that the development of tailored design guidelines for CRM is necessary.

For this purpose, both academic and industrial research have significantly contributed not only to the development of CRM systems (through laboratory tests on small-scale specimens, such as tensile tests on meshes and coupons, shear bond tests, and pull-out tests), but also to the investigation of their effectiveness for the structural rehabilitation of masonry. These studies have been mainly conducted through tests on medium-to large-scale structural elements (e.g., panels subjected to in-plane and out-of-plane loading, floor strips, arches, and vaults), as well as full-scale building experiments and have provided valuable insights for design applications. The investigations described in the literature include quasi-static tests with monotonic or cyclic loads, and dynamic/seismic tests using shake tables, and employ a wide range of setups and displacement measurement technologies. Specific references are listed hereinafter in the dedicated chapters of this paper. It is worth noting that the number of articles indexed in major databases (e.g., Scopus, Web of Science) has grown exponentially, from fewer than 10 per year between 2000 and 2012, to an average of around 50 per year since 2018. This trend, alongside a similar increase in publications in specialized journals for practitioners, demonstrates the growing interest CRM systems have generated in the research, manufacturing, and engineering communities. Despite scientific evidence provides a sufficiently extensive body of work demonstrating the effectiveness of CRM systems, the knowledge developed so far has remained fragmented. This has hindered a clear and shared identification of the areas that still require investigation, from both experimental and theoretical standpoints. Furthermore, the absence of validated analytical formulations and design criteria has, to date, limited the adoption of CRM in engineering practice.

To advance the technical and scientific knowledge on the mechanical behaviour of CRM systems and of structural elements strengthened with this technology, and to promote an informed application in the field of structural rehabilitation, it is now necessary to:

(i) Compile a state-of-the-art review of the experimental evidence available in the scientific literature, in order to thoroughly understand the mechanical response of CRM systems, assess their effectiveness in enhancing the structural capacity for the various possible applications, and establish the current level of knowledge in this specific field;
(ii) Collect experimental test databases in an organized and consistent form, suitable for the development, validation, and calibration of numerical models for simulating the structural behaviour of masonry elements strengthened with CRM;
(iii) Compile a state-of-the-art review of the analytical models proposed in the literature for the theoretical estimation of the ultimate strength of structural elements retrofitted with CRM, discuss their reliability in order to identify formulations suitable for design purposes, which need to be validated and calibrated against experimental evidence in order to be effectively employed in professional engineering practice;
(iv) Identify the areas in which further knowledge is required and that therefore demand additional scientific research efforts.

This paper provides an overview of the experimental investigations carried out on CRM systems, including durability assessments, as well as on structural members retrofitted with CRM, specifically, masonry walls under in-plane shear loading, masonry walls subjected to out-of-plane bending, crowning beams, and vaulted structures. For each strengthening application, dedicated databases compiling the corresponding experimental results are presented. Construction details and on-site installation procedures are discussed whenever experimental evidence is available.

The capacity models proposed in the literature for estimating the strength of retrofitted structural elements are also reviewed, and the conditions under which these models provide the most accurate strength predictions are critically discussed. Furthermore, the paper explores the latest technologies combining structural reinforcement with energy efficiency, such as the use of high-performance mortar matrices for thermal-acoustic insulation. Lastly, it describes the effectiveness shown by CRM systems for seismic retrofitting, even when consisting of one-sided interventions aimed at minimizing the invasiveness, preserving decorated surfaces, or maintaining fair-faced masonry, which is required by applications to architectural heritage.

Applications to columns are instead excluded since CRM is unsuitable for confinement. The lower tensile stiffness of the FRP meshes used for CRM composites compared to that of carbon and steel textiles used in organic and inorganic matrix-based composites makes these latter technologies currently preferable over CRM for confinement. Moreover, the pre-cured L-shaped corner mesh elements included in CRM kits can be used to ensure continuity of the reinforcement across building corners (adequate overlaps are needed) but are not designed to sustain the tensile stresses expected in confining overlays.

Although a comparative economic assessment does not fall within the scope of this work, it cannot be overlooked that the application costs of CRM systems significantly influence the widespread adoption of this technology within a market context where the main competing solutions are FRP and FRCM systems. In practice, the overall installed cost of strengthening interventions is strongly affected by several factors, including the type and weight of the reinforcing mesh or fibres, the number of layers, the thickness of the mortar matrix, the condition and accessibility of the substrate, site-specific constraints, local regulations, and the total extent of the intervention. Based on current practice and available cost assessments, FRP systems generally fall within a range of 80-250€/m^2 when expressed per unit area. However, this metric can be misleading because FRP reinforcements are typically applied in a discrete manner (strips, laminates, or bars placed only where needed) so their actual incidence per square meter of wall surface is often significantly lower than that of surface-distributed systems. FRCM solutions, by contrast, are applied as continuous layers over the entire surface and therefore exhibit more directly comparable areal costs, typically around 60-200€/m^2, reflecting the use of inorganic matrices and installation procedures like traditional plastering. CRM systems also involve full-surface application but require thicker mortar layers, mechanical connectors, and longer installation times; as a result, their overall costs commonly range from about 200 to 400€/m^2.

It should be noted that these considerations ideally refer to strengthening solutions designed to achieve comparable structural performance targets, such as similar increases in shear or flexural capacity, consistently with cost-benefit approaches available in the literature [19]. Although rigorous quantitative assessments would require case-specific structural analyses and detailed bill-of-quantities evaluations, FRP systems generally require smaller material quantities but involve higher unit costs, whereas FRCM and CRM systems rely on full-surface applications characterized by lower material costs but higher labour incidence. Systematic studies directly comparing the cost effectiveness of the different strengthening techniques are still not available in the scientific literature, but in construction price lists (see, for instance, Ref. [20]) CRM interventions are associated with the abovementioned higher unit costs due to thicker mortar layers and the use of mechanical connectors.

Within this framework, a systematic and critical organization of the available knowledge appears essential to bridge the gap between experimental evidence, analytical modelling, and engineering practice, and also the techno-economic considerations that influence the selection among different strengthening strategies. The absence of consolidated and CRM-specific design guidelines further reinforces the need for a structured synthesis of existing research outcomes, not only in terms of mechanical performance but also with respect to practical implementation aspects. Accordingly, the following sections provide a reference framework for both researchers and practitioners, supporting the interpretation of experimental evidence and facilitating the development of practice-oriented methodologies for the applications to CRM systems to masonry structures.

2. Material properties

2.1. Mechanical characterization tests and certification protocols

In the case of CRM strengthening systems, the main geometric properties of the meshes are the grid spacing and the cross-sectional area of each fibre bundle, which must be specified separately in the warp and weft directions for unbalanced meshes. More rarely, reference is made to the equivalent thickness of the mesh, defined as the net cross-sectional area of fibres per unit width of the textile (t_f), which is, instead, the universally adopted practice for textiles used in FRCM composites. Concerning mechanical properties, the main parameters of the mesh are the tensile strength (f_f) and the tensile modulus of elasticity (E_f). The tensile response is typically linear-elastic up to brittle failure. Strength and stiffness are generally referred to the cross-sectional area of the individual fibre bundle (which includes the impregnating resin), whereas only in rare cases are they expressed with respect to the net area of the fibres alone. Such mechanical properties may differ between weft and warp, even for balanced meshes, since the industrial manufacturing process,

Fig. 2. Experimental setups of direct tensile tests on mesh bundles (a) and CRM coupons (b), of pull-out tests (c), and of shear bond tests (d).

based on mechanical weaving looms, typically produces a grid in which the weft consists of flat, parallel fibre bundles, whereas the warp is formed by two twisted fibre bundles wound around each other to enable an effective stitching at the intersections between weft and warp (Fig. 1a).

Certification protocols have been developed in the EU [14] and in Italy [15] to establish standardized criteria for testing CRM systems and obtaining the ETA (European Technical Assessment, EU) or CVT (Certificato di Valutazione Tecnica, Italy) certifications required for their commercialization and use in structural strengthening. Both standards require laboratory tests to be performed only on the FRP mesh, on the FRP mesh corner elements, and on the mechanical connectors that provide mesh-to-substrate stress transfer. These tests include direct tensile tests, which determine the tensile strength and the tensile modulus of elasticity (Fig. 2a); pull-out tests on connectors, used to assess their pull-out resistance from standardized substrate materials (Fig. 2c); and tensile tests on connector overlaps, which evaluate the connector-to-connector stress-transfer capacity along a specified overlap length (transverse connectors may consist of two elements inserted from opposite sides of the wall). For each test type, 9 specimens are to be tested. Durability tests are also required on specimens aged in alkaline or saline solutions, high humidity, or subjected to freeze-thaw cycles. In all these cases, testing is carried out exclusively on the FRP components of CRM systems.

Conversely, certification protocols do not require testing of the mortar matrices. Any mortar certified for structural use is deemed suitable for CRM applications. This approach is consistent with that adopted for more traditional construction materials, including those used for structural retrofitting (for example, steel meshes and mortars/concretes employed in reinforced plaster systems), yet differs from the certification procedures prescribed for FRP [21] and FRCM/TRM [22,23] composites. Limiting testing to the FRP components of CRM systems streamlines the certification process, since composite specimens do not need to be fabricated, cured, and tested in the laboratory, which would be time-consuming and costly. It also allows CRM systems to incorporate a much wider range of constituent materials, because the FRP components and mortars do not need to be supplied by a single manufacturer.

Experimental studies available in the literature, either specifically focused on the mechanical behaviour of FRP meshes used in CRM strengthening systems [24–27] or conducted as part of broader experimental programmes on strengthened structural elements, consistently report comparable ranges of mechanical properties. Tensile strength values (f_f) typically fall between 1000 MPa and 1500 MPa, while the tensile modulus of elasticity (E_f) ranges from 55 GPa to 75 GPa. Peak strain measurements are generally reported between $10 \cdot 10^{-3}$ and $22 \cdot 10^{-3}$. These data are obtained from direct tensile tests performed on single bundles extracted from the FRP mesh (Fig. 2a), on specimens consisting of two or three bundles, and, less frequently, on CRM composite prismatic specimens (coupons, Fig. 2b). In these investigations, to ensure uniform stress transfer at the load introduction areas, metallic or composite tabs were bonded to the ends of mesh specimens, while FRP wraps were applied along the edges of coupons.

Few experimental studies exist that have also examined the bond between CRM composites and masonry substrates, following approaches typically adopted for FRCM systems [25,27] (Fig. 2d). From a design perspective, the contribution of the matrix-to-substrate bond cannot be regarded as uniformly secondary. Its effectiveness depends strongly on the relative in-plane stiffness of the CRM layer and the underlying masonry. When this stiffness mismatch is large, premature debonding may occur under in-plane loading, making the role of mechanical connectors crucial for ensuring reliable load transfer. Local stress concentrations, as well as long-term effects associated with cyclic loading or temperature variations, may also contribute to bond degradation. Conversely, as the stiffness of the CRM layer approaches that of the substrate, the bond mechanism may become progressively more effective, reducing the demand on the connectors and allowing a more distributed transfer of stresses across the interface.

No experimental investigations are currently available in the scientific literature for the mechanical characterisation of meshes used in CRM strengthening systems that incorporate fibres other than glass.

An innovative contribution to the mechanical characterization of CRM materials was recently provided by De Santis and co-authors [27] and consisted of the development of self-sensing systems, in which Fibre Bragg Grating (FBG) sensors are embedded within a glass FRP mesh to enable simultaneous strengthening and monitoring. Experimental investigations included direct tensile tests on fibre bundles and CRM coupons, shear bond tests on CRM-to-masonry interfaces, and pull-out tests on GFRP connectors, and confirmed the outcomes of previous studies dealing with the mechanical testing of CRM constituents, but, in addition, demonstrated the ability of FBGs to capture strain evolution, detect early damage phenomena such as cracking, slippage, and interface degradation, and monitor load redistribution during progressive failure.

2.2. Design values of mechanical properties

According to Eurocodes, as well as to the scientific and technical literature, the design values of the mechanical properties of construction materials are derived from the results of laboratory characterization tests carried out in accordance with certification standards, while accounting for expected uncertainties, variability, and long-term effects. Even remaining only within the field of innovative composite materials for structural strengthening that are close to CRM, this is the same approach already recommended for organic-matrix composites [28], inorganic-matrix composites [17], and even for FRP bars used as internal reinforcement in concrete structures [29]. To date, however, a design guide for CRM systems has not been developed, so no shared indications are currently available for determining the design values of the mechanical parameters to be used in ultimate limit state and service limit state calculations.

For design purposes, the main mechanical parameters are the tensile modulus of elasticity and the tensile strength (or strain), assuming that a linear elastic constitutive behaviour up to a brittle failure can be adopted. The nominal value of the tensile stiffness corresponds to the average value obtained from direct tensile tests. Regarding strength, the characteristic value (5% fractile) is calculated as the mean minus twice the standard deviation [14], following the design-by-testing approach recommended in Annex D of Eurocode 0 [30], considering that nine specimens are tested in direct tension for mechanical characterization [14].

The design value of the ultimate strength is then obtained by dividing the characteristic value by an appropriate partial safety factor, which should be calibrated based on the variability of test results. To establish such a factor, existing investigations should be compiled and statistically analysed, a task that clearly deserves targeted research initiatives in the near future. Additionally, an environmental reduction factor should be applied to account for long-term degradation. Durability tests are required to calibrate this factor under various aggressive exposures. Limited knowledge is currently available on this specific aspect, although recent studies promoted within international scientific committees, such as RILEM TC 290-IMC, have begun to address it. Further information may also be extracted from tests conducted by manufacturers for product certification, which should be collected and analysed.

As a preliminary approach, and until specific calibrations and dedicated investigations on CRM systems are available, the values adopted for externally bonded glass FRP composites are generally adopted. These include a partial safety factor of 1.3 and environmental reduction factors of 0.75, 0.65, and 0.50 depending on the exposure conditions (indoor, outdoor, aggressive).

2.3. Durability tests

Even though CRM systems have been increasingly adopted for the strengthening of masonry structures over the past two decades, durability has emerged as a key factor governing long-term effectiveness only in recent years, thus remaining a major concern. The durability of CRM is influenced by the chemical nature of its constituents and by the interactions among reinforcement, mortar matrix, and substrate, as well as by environmental exposure conditions. The scientific research has investigated some of these aspects, partially building upon the knowledge previously developed for FRP and FRCM systems, at least from a methodological standpoint. Experiments relied on the accelerated aging protocols already used for these other composites, including exposure to alkaline or saline solutions, freeze-thaw cycles, salt fog, and hygrothermal conditioning. On the other hand, while some experimental findings derived from FRP and FRCM provide valuable insights also for CRM, primarily those on the tensile strength of the mesh retained after aging, fundamental differences in terms of technology and structural functioning require dedicated experimental investigations, e.g., with reference to the role played by the properties of the mortar matrix and to the long-term connector-to-substrate bond properties.

The most significant studies have focused on the behaviour of the FRP meshes, investigated through laboratory tests performed on artificially aged specimens. Glass fibres, which are the most widely adopted in CRM systems, have been extensively studied due to their potential susceptibility to alkaline attack, which is first of all constituted by the mortar matrix. Alkali-resistant (AR) glass fibres showed better performances than E-glass, but, if not adequately protected, exposure to alkaline attack may lead to strength degradation over time even in AR glass [26,31].

As regards other fibre materials, basalt exhibits improved chemical stability compared to conventional E-glass, but its long-term performance under alkaline and wet conditions remains a primary concern [32]. Carbon exhibits excellent resistance to alkaline environments, moisture, wet-dry, and thermal cycles, resulting in superior durability performance [33], but its higher cost is currently the main obstacle to its wider adoption in CRM systems, also considering that most structural applications do not require fully exploiting its higher tensile strength and stiffness compared to glass and basalt.

In this area, a key contribution was provided by an extensive experimental study conducted in Ref. [26], assessing the residual tensile strength of different fibres, including E-glass, AR-glass, basalt, PBO, carbon, and steel, after exposure to multiple alkaline aging protocols. Both dry and impregnated fibres were tested in cementitious and lime-based environments, totalling nearly 800 tensile tests. Results showed significant differences in chemical resistance. E-glass and basalt fibres were highly susceptible to degradation, whereas AR-glass maintained strength reductions generally within 20%, and carbon and steel fibres exhibited negligible loss. SEM analyses revealed the initiation and progression of chemical attack at the fibre surface. The study highlighted the importance of considering the type and concentration of alkaline species, the accelerating role of temperature, and the need for dedicated aging protocols and quantitative criteria for the qualification of FRCM/CRM systems. In a follow-up investigation, CRM proved to retain a significant portion of its mechanical capacity after aging even under high-temperature exposure, with degradation rates markedly lower than those observed in FRP composites [34].

The role of the mortar matrix and the associated stress-transfer mechanisms is a critical aspect for the durability and long-term effectiveness of mortar-based composites, particularly in FRCM. In these systems, the reinforcement is typically provided in the form of dry, coated, or partially impregnated textiles. As a consequence, the porosity, tensile strength, cracking susceptibility, and permeability of the mortar matrix play a key role in controlling durability, because they can lead to the direct exposure of the fibres to aggressive agents originating from the substrate or the external environment. In contrast, in CRM, the influence of the mortar matrix is comparatively less pronounced because the fibres of the reinforcing FRP mesh are fully embedded within a polymeric matrix, inherently providing enhanced protection against chemical and environmental attack.

A similar distinction applies to the role of adhesion mechanisms. While the structural efficiency and durability of FRCM systems strongly depend on the quality and stability of the textile-to-matrix and matrix-to-substrate bond, mechanical connectors are systematically used in CRM applications to ensure effective stress transfer between the FRP mesh and the structural element. This significantly reduces the sensitivity of CRM systems to degradation phenomena affecting adhesive interfaces, thereby enhancing robustness and durability under long-term environmental exposure and sustained loading conditions [35].

Time-dependent phenomena such as creep, shrinkage, and stress relaxation are expected to play a non-negligible role in the durability of CRM-strengthened members. The mortar matrix exhibits viscoelastic behaviour under sustained stress, potentially leading to stress redistribution between fibres and matrix over time. Sustained loading combined with environmental exposure can amplify degradation effects, particularly in systems with lower fibre volume fractions. Although creep effects in CRM systems are theoretically lower than those observed in polymer-based composites at elevated temperatures, their influence on serviceability and crack control requires further investigation, especially in long-span or heavily loaded structural elements.

With regard to high-temperature exposure, one of the most significant advantages of CRM systems lies in their superior performance under fire conditions over FRP, thanks to the presence of the mortar matrix, which protects the embedded FRP mesh, and FRCM, thanks to the larger thickness. Additionally, CRM composites do not rely on organic resins (whose mechanical properties degrade rapidly at relatively low temperatures) to ensure the load transfer with the substrate and include a layer of mortar. Experimental campaigns (on FRCM) have demonstrated that members strengthened with inorganic matrix composites retain a substantial portion of their load-carrying capacity after exposure to temperatures exceeding 400-600 $^{\circ}$C, depending on fibre type and matrix composition [36,37]. Thermal compatibility between matrix and substrate further enhances durability by limiting thermally induced stresses and debonding phenomena. Even if specific studies on CRM have not been conducted so far, these characteristics suggest that CRM systems are particularly suitable for applications where fire resistance and post-fire functionality are critical design requirements.

At the current state of the art, the growing body of experimental evidence has provided some information on the long-term behaviour of CRM systems and has supported the development of certification standards [14], in which, building on the knowledge already established for FRP and FRCM, durability is a key aspect. Several challenges, however, remain open. First, additional experimental investigations are required that consider a wider range of constituent materials and investigate their behaviour under different aging scenarios and exposure conditions. Increasing the number and diversity of experimental evidence is essential to improve the understanding of degradation phenomena, to guide industrial development toward increasingly durable CRM systems, and to provide a statistically robust basis for the definition of durability-related coefficients (environmental reduction factors) to be introduced into design standards. Ultimately, the availability of a broader and more reliable experimental database would enable the refinement and calibration of artificial aging protocols currently prescribed in certification standards, leading to more representative and effective laboratory procedures for durability assessment. Future research is also expected to combine experimental, analytical, and numerical approaches, focusing on multiscale modelling of degradation mechanisms, probabilistic durability-based design, and the development of digital tools for predicting residual performance over the service life.

2.4. Compatibility issues

The great flexibility arising from the possibility of combining different certified FRP meshes with mortar matrices places increased emphasis on the assessment of compatibility both among the constituent materials of the CRM system and between the CRM system and the existing substrate. Although no specific requirements addressing these aspects are provided in the current standards, experimental studies have highlighted that the interaction among mesh, mortar and substrate influences the structural response and long-term effectiveness of CRM-strengthened masonry elements [38,39]. Therefore, several aspects deserve careful consideration during the material selection phase.

First, the rheological and granulometric characteristics of the mortar affect its penetration around the mesh yarns and nodes, governing stress transfer mechanisms and the effectiveness of the mechanical interlock developed at the interface [35]. Mechanical interaction between the mesh and the mortar is generally enhanced when the mesh is produced by interweaving continuous fibres at the nodes, whereas thermally bonded meshes may exhibit reduced load transfer efficiency and increased susceptibility to slip. These mechanisms may also be influenced by the presence of short dispersed fibres within the matrix [40].

Second, from a chemical standpoint, the durability of the mesh, despite the use of alkali-resistant (AR) fibres and epoxy impregnation, as well as that of the fibre-to-matrix interface, may be affected by prolonged exposure to alkaline environments [26,31]. This highlights the importance of chemical compatibility between the FRP mesh and the matrix, whose composition and alkalinity may play a significant role in governing the long-term durability of the composite system. The high pH, which may range from approximately 12 to 14 depending on the mortar composition and curing stage, can promote the attack of OH^{-} ions on glass and basalt fibres, leading to hydrolysis and progressive degradation. Even limited surface damage induced by alkaline corrosion may result in a reduction in fibre tensile strength [26].

As regards compatibility with the substrate, adequate interaction between the mortar matrix and the masonry is required to minimize stiffness mismatch and localized stress concentrations, particularly in heritage structures characterized by low-strength materials. Finally, when CRM systems are employed for the strengthening of historic masonry, natural hydraulic lime (NHL)-based mortars are often preferred owing to their physical, chemical and mechanical compatibility with traditional construction materials, as well as their favourable hygrothermal behaviour, which helps prevent moisture accumulation within highly porous masonry substrates [39].

3. In-plane strengthening of masonry walls

3.1. General considerations

Masonry walls are subjected to in-plane shear loads mainly due to earthquakes and typically develop diagonal cracking. At the onset of ground motion, small lateral displacements may cause fine cracks to form near openings, where stress concentrations are present. As shaking increases, these cracks extend following a diagonal path, generally at about 45°, from the corners of openings or from the wall base. Cyclic loading leads to the formation of a second diagonal crack, producing the typical shear-induced X-shaped crack pattern. With increasing demand, these cracks widen, mortar joints progressively degrade, and localized crushing or dislodgement of units may occur, indicating the approach to shear failure.

Besides this typical shear collapse mechanism, an in-plane bending mechanism may also occur (for example, in slender elements under low axial stress). This phenomenon mainly involves the element extremities, where the bending moment is higher, activating cracking of the cross-section on one side and crushing of the masonry on the opposite side. Cyclic loading leads to alternating cracking and crushing on opposite sides, and a sliding mechanism along the cracked mortar joints may also occur.

The need to protect the built heritage in seismic-prone areas and to upgrade the in-plane capacity of walls under earthquake-induced shear damage has significantly stimulated research efforts. In this context, experimental studies on large-scale masonry wall prototypes subjected to in-plane loads saw substantial development in the late 1990s, aiming to predict the shear behaviour of masonry and to identify suitable strengthening techniques for constructions damaged by earthquakes. Tests have been conducted both in the laboratory and in situ, improving the understanding of masonry mechanical properties, which is essential for assessing seismic vulnerability and designing effective retrofit interventions.

CRM systems have demonstrated their ability to enhance the coupling of the compressive strength of masonry with the tensile capacity of a reinforcing mesh. This combination provides the wall with increased resistance to cyclic lateral loads, limits cracking, and prevents brittle failure. CRM overlays can be applied to one or both faces of the wall. Their application over the entire wall surface ensures a distributed strengthening effect and prevents masonry disaggregation. Moreover, transverse connectors ensure effective load transfer between the CRM system and the masonry substrate, and prevent leaf separation in multi-leaf walls.

3.2. Experimental evidence

The effectiveness of CRM for improving the strength and deformation capacity of masonry walls has been investigated through laboratory diagonal compression tests and shear-compression tests. Among the testing procedures, the diagonal tension test, standardized by ASTM 519 [41], is the most commonly used. In this test, the shear load is applied along one diagonal of a square masonry panel by means of a hydraulic actuator, and failure typically occurs through the formation of a diagonal crack initiating near the panel centroid, where the principal tensile stresses are highest. This test configuration allows for the determination of the shear strength of masonry by loading the panel in compression along its diagonal (Fig. 3a). An additional advantage of the diagonal tension test is that it can also be performed in the field, by extracting a square masonry panel from the structure.

Several experimental studies have been carried out over the past 15 years to quantify the increase in shear strength, ductility, and energy dissipation provided by CRM applied to masonry walls. Compared with other applications, such as the out-of-plane flexural strengthening of walls or the retrofitting of vaulted structures, the use of CRM for in-plane strengthening has received predominant attention in the scientific literature.

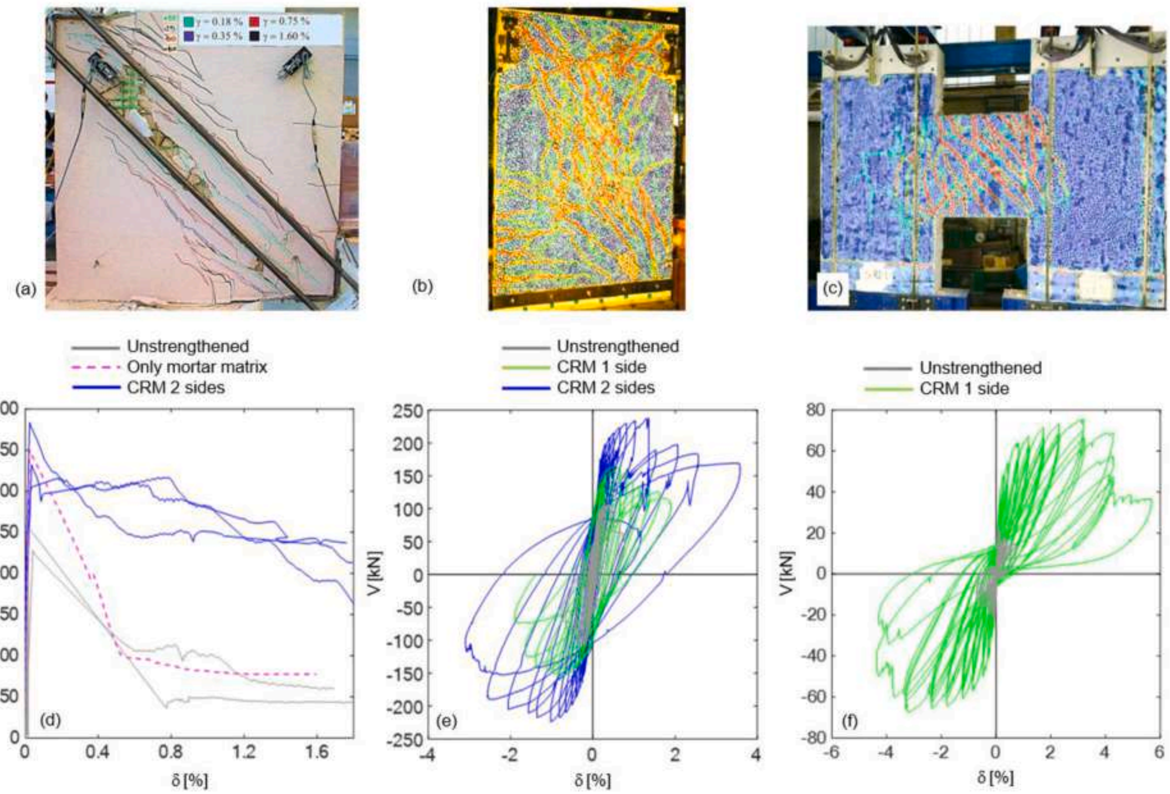

Fig. 3. Crack patterns (a-c), highlighted by DIC strain fields when available (b,c) and response curves (d-f) of masonry specimens strengthened with CRM: diagonal compression tests on masonry walls [38] (a,d), compression-shear tests on masonry piers [42] (b,e), and bending-shear tests on masonry spandrels [43] (c,f).

The first study was carried out in Ref. [44]. The authors conducted an extensive investigation on wall panels of solid double-headed, triple-headed, and multi-leaf brickwork with a weak inner core of loose material, as well as roughly squared stone masonry, all reinforced with a plaster layer embedding a GFRP mesh. Diagonal compression tests demonstrated the effectiveness of the CRM system across all masonry types, with shear strength approximately doubling for double-headed brickwork and tripling for roughly squared stone. All strengthened configurations exhibited improved ductile behaviour, showing a gradual reduction in strength while retaining significant residual capacity even at large deformation levels.

Four years later, Corradi and colleagues [45] tested wall panels extracted from three historic Italian buildings, two constructed with rubble stone masonry and one with solid brick masonry, which underwent diagonal compression and combined shear-compression tests. The results showed a substantial increase in shear strength after jacketing, with strengthened specimens achieving lateral loads more than an order of magnitude higher than the unstrengthened panels. In addition to strength enhancement, the retrofitted panels exhibited improved ductility and energy dissipation. These benefits were attributed to the effective interaction between the GFRP mesh and the mortar matrix, which promoted a more uniform stress distribution and delayed the onset of failure mechanisms typically observed in unstrengthened masonry.

A subsequent work by Gattesco and Boem [38], carried out in the wake of [44], compiled experimental results to evaluate the CRM system for different masonry typologies, namely solid brick, cobblestone, and rubble stone, and for panels with varying thicknesses. Reference and strengthened specimens were tested, the latter retrofitted with a GFRP mesh embedded in different mortar types applied on both wall faces. The results confirmed substantial increases in shear strength and ductility due to the strengthening intervention. Importantly, the effectiveness of the system was found to be only marginally influenced by the mechanical strength of the mortar coating.

After these pioneering studies, more research has been conducted to assess the gain in strength and ductility provided by CRM composites on masonry walls loaded in their plane, to investigate the role played by mesh architecture and mortar properties, the effectiveness of mechanical connectors for preventing bond-related failure modes, the extent to which CRM overlays applied only to one wall side offer performance comparable to symmetric double-sided configurations, and even the effect of high temperatures.

In the investigation presented in Ref. [46], masonry wall prototypes constructed using a two-leaf bond with clay bricks were retrofitted with a CRM system embedding a GFRP mesh. Significant improvements in shear strength, ductility, and stiffness were observed. Further diagonal compression tests in Refs. [47,48] confirmed these results. In this case, several CRM systems using the same mortar, but different FRP meshes, namely basalt, glass, and carbon, were tested on solid brick and insulated concrete masonry walls. All systems proved effective in enhancing shear strength and deformation capacity, although the basalt mesh showed only minimal improvement in strength and ductility. The analysis of failure modes indicated that the mesh-matrix interface was the weakest link in the system.

The experimental study described in Ref. [49] focused on ten clay brick masonry panels with two CRM configurations tested under diagonal compression. Results showed improved shear capacity and ductility, particularly when CRM was applied to both wall surfaces. Panels retrofitted on only one side were more susceptible to out-of-plane instability and showed reduced strength. The study in Ref. [40] examined how reinforcement configuration, cement content in the matrix, and mesh type (steel and GFRP with 30mm $\times$ 30 mm and 40mm $\times$ 40 mm spacing) influenced performance. Shear capacity nearly doubled when CRM was applied to both sides. Higher cement content led to significant improvements in strength, stiffness, and energy dissipation. Among the mesh types, the wider GFRP mesh was the most effective, highlighting the importance of both geometric and mechanical mesh properties. The increase in shear strength provided by CRM was confirmed by the tests conducted by D'Antino and co-authors [50], carried out on brickwork panels extracted from an early-twentieth-century building.

Over the past few years, a broader comparison was made of CRM systems with different mortars, mesh types, and connector configurations in Ref. [51]. Diagonal compression tests on stone masonry panels showed the most significant improvements with high connector densities. Increasing mortar strength also correlated with better performance, while mesh type and connector type showed no significant influence. Ponte and co-authors [52] investigated rubble stone masonry typical of historic buildings in Southern Portugal and other Mediterranean regions. Panels strengthened on one face with either carbon or glass mesh were tested under cyclic loading with cantilever boundary conditions. Both systems yielded similar performance, although the full potential of the carbon mesh was not fully realized.

In [37], the effects of high temperature (600 °C) were studied on masonry wall panels retrofitted with carbon and glass CRM, tested before and after thermal exposure. At room temperature, CRM systems improved their strength and ductility. Post-fire tests showed that carbon CRM, when applied after heating, restored both strength and stiffness and improved ductility. Glass fibre systems performed worse, primarily due to lower mesh durability. When CRM was applied before heating, carbon meshes still restored strength but not stiffness, while specimens retrofitted with glass meshes behaved similarly to the unstrengthened ones. Debonding occurred in the latter case, indicating the need for further investigation into connector use to improve post-fire bonding performance.

Attention to sustainability has driven part of the research on innovative composites, such as CRM for the rehabilitation of existing structures, either by selecting low-impact materials (natural or recycled) or by integrating structural and energy upgrades. In Ref. [53], the authors evaluated a CRM system using hemp fibres combined with two types of mortar, applied to panels made of Neapolitan yellow tuff and solid clay bricks. The results highlighted the effectiveness of the reinforcement system, which provided performance comparable to commercial solutions while offering a more sustainable alternative. In a follow-up study [54], the same research group compared the performance of hemp fibre meshes with that of conventional GFRP meshes. The hemp-retrofitted panels showed greater strength increases, with failure occurring due to mesh rupture. In contrast, the GFRP- retrofitted specimens exhibited debonding, likely due to the higher axial stiffness of the glass fibres. High ultimate deformation values were achieved in all cases, especially in panels retrofitted with thinner plaster layers. An example of integrating thermal and structural performance is given in Ref. [55], in which four different CRM systems were tested using various mortar types, including thermal-insulating mortars. Mechanical and thermal testing confirmed the feasibility of this solution. In Ref. [56], the authors investigated walls made of sharp limestone blocks and weak hydraulic mortar, retrofitted with systems that included recycled fine aggregates from limestone cutting waste. The strengthening improved the load-bearing capacity and altered the mechanical behaviour, including failure modes and strain-energy retention, thereby preventing the complete disintegration of the masonry panels. Lastly, the campaign in Ref. [57] studied CRM systems as dual-purpose retrofitting solutions for both thermal and seismic improvement. Two mortar types were tested, traditional lime-based and geopolymer-based, against conventional techniques. Both improved shear strength and modulus, with the lime-based system showing higher strength and the geopolymer system yielding greater ductility. More details on the integration of structural and energetic upgrades are provided in Section 8.

Some investigations compared CRM with other mortar-based composites. The authors in Ref. [58] compared CRM with FRCM systems through diagonal compression tests on clay brick panels. CRM systems exhibited less widespread cracking and a greater sensitivity to mortar properties, likely due to the wider mesh and thicker mortar. The increased matrix thickness also contributed to higher load capacities. CRM-retrofitted panels demonstrated more ductile behaviour and higher initial stiffness. In Ref. [59], the effectiveness of a glass mesh versus a balanced basalt-stainless steel mesh was tested on clay brick panels. The former used a lime-based mortar, while the latter used a lime mortar with mineral binders. Both systems were effective, although GFRP yielded higher peak loads, whereas the basalt-stainless-steel mesh provided greater ductility.

The experimental evidence confirms the effectiveness of CRM systems in enhancing the structural performance of masonry walls, particularly in terms of in-plane shear strength, ductility, and post-peak energy dissipation. The results are consistent across various masonry typologies and configurations, highlighting the adaptability of the technique. While glass and carbon mesh are commonly used, alternative materials such as hemp fibres also show promising outcomes, particularly for sustainable retrofitting applications. The performance of the CRM system is influenced by several parameters, including mesh type and spacing, mortar composition, strengthening configuration (single-versus double-sided), and the presence of mechanical connectors. Furthermore, CRM systems have demonstrated potential for post-fire repair and combined thermal-structural retrofitting when used with insulating mortars. Despite some limitations, such as potential bond weakness at the mesh-matrix interface, CRM proves to be a practical and efficient solution for preserving and seismic upgrading existing masonry structures. Future research should focus on optimizing bond performance, evaluating long-term durability, and developing integrated approaches that address both structural and energy-related requirements.

As regards progressive damage development, experiments have shown that it is governed by a sequence of interacting mechanisms that reflect both the behaviour of the masonry substrate and the contribution of the CRM system. Initial cracking typically occurs within the masonry, often along mortar joints or pre-existing weaknesses, as the panel undergoes shear deformation under increasing load. As the stress level increases, cracks propagate and progressively activate the reinforcing mesh embedded in the mortar layer, which begins to carry tensile forces and redistribute stresses over a wider area compared with the typical response of unstrengthened masonry (Fig. 3a). With further in-plane loading, the system enters a more complex phase in which the masonry substrate and the CRM layer interact, though not always in perfect compatibility. Local debonding or partial detachment between the mortar matrix and the masonry may occur, particularly near pre-existing cracks or along panel edges, reducing the effectiveness of tensile stress transfer. The reinforcing mesh may consequently experience localized strain concentrations, potentially leading to progressive rupture of individual fibres or bundles, even though this phenomenon is rarely observed in laboratory tests. Overall failure typically results from the combined action of these mechanisms rather than from a single abrupt event. The panel usually exhibits a global multi-diagonal cracking pattern along the compressed diagonal direction, which continues to develop until the strengthening system is no longer able to sustain the imposed tensile stress demand (Fig. 3a–c).

The experimental response curves are inherently and strongly influenced by the specimen geometry, the mechanical properties of the masonry substrate, and the layout of the applied strengthening system, as well as by the boundary conditions and the presence of an axial compressive load. Fig. 3d–f provide representative examples of the comparison among response curves obtained from diagonal compression tests (Fig. 3d, [38]), shear-compression tests on masonry piers (Fig. 3e [42]), and shear-flexure tests on spandrel elements (Fig. 3f [43]). The drift values (δ) reported on the horizontal axis and the shear (V) reported on the vertical axis cannot be directly compared in quantitative terms, as they refer to experimental campaigns carried out on different masonry prototypes and employing different CRM configurations.

Nevertheless, the overall shapes of the curves highlight a fundamental difference in structural behaviour. In the case of diagonal compression tests (relatively easy and cheap to carry out, which provide a general evidence of the reinforcement benefits), the specimens exhibit a stiff initial response up to the attainment of a peak load, typically associated with cracking and crushing of the mortar matrix, followed by a progressive post-peak strength degradation, in which the FRP mesh predominantly carries the applied load. This behaviour is further evidenced by the fact that the prototype strengthened solely with mortar overlays attains peak load levels comparable to those of the specimen reinforced with a complete CRM system, while exhibiting a much more rapid degradation of load-carrying capacity in the post-peak regime (Fig. 3d). Conversely, shear-compression and shear-flexure tests (more complex and expensive to perform, but which reproduce more realistically the actual configurations) are characterised by a less brittle response. In these tests, the presence of CRM strengthening leads not only to an increase in the maximum shear resistance, but also to a pronounced enhancement of displacement capacity and of the ability to withstand large drift demands over repeated loading cycles (Fig. 3e and f). Lastly, the shear-compression tests on masonry piers described in Ref. [42] indicate that a CRM system applied to only one side of the wall, although resulting in a response that appears essentially similar in the positive and negative quadrants of the plot, leads to reduced capacity both in terms of maximum shear and ultimate drift when compared to symmetrically CRM configurations (Fig. 3e). However, the increase in performance is significant compared to the unreinforced configuration.

Table 1 summarizes the experimental data on masonry walls strengthened with CRM under shear loading (data curated according

Table 1
Summary of the experimental results of in-plane shear tests on masonry walls.

Ref.	Masonry wall specimen [a]			CRM system [b]									Results	
	Label	t_w [m]	$f_{c,URM}$ [MPa]	t_m [mm]	f_{cm} [MPa]	f_{tm} [MPa]	Fib.	GS [mm×mm]	t_f [mm²/m]	f_f [MPa]	E_f [GPa]	TC	τ_0 [MPa]	τ/τ_0 [−]
[44]	MT-1A-F33S	0.38	11.5	30	7.8	1.56	G	33×33	0.348	897	23	Y	0.47	1.64
	MT-1A-F66S	0.38	11.5	30	7.8	1.56	G	66×66	0.174	963	23	Y	0.47	1.65
	MT-1A-F66SL	0.38	11.5	30	7.8	1.56	G	66×66	0.174	963	23	Y	0.47	1.92
	MP-1A-F33S	0.40	1.45	30	7.8	1.56	G	33×33	0.348	897	23	Y	0.20	2.85
	MP-1A-F66S	0.40	1.45	30	7.8	1.56	G	66×66	0.174	963	23	Y	0.20	2.66
	MP-1A-F66D	0.40	1.45	30	7.8	1.56	G	66×66	0.348	760	27	Y	0.20	3.08
	MD-1A-F33S	0.25	11.5	30	7.8	1.56	G	33×33	0.348	897	23	Y	0.47	1.98
	MD-1A-F66S	0.25	11.5	30	7.8	1.56	G	66×66	0.174	963	23	Y	0.47	2.06
	MD-1A-F99S	0.25	11.5	30	7.8	1.56	G	99×99	0.116	586	23	Y	0.47	2.14
	MD-1C-F33S	0.25	11.5	30	7.8	1.56	G	33×33	0.348	897	23	Y	0.63	1.62
	MD-1C-F66S	0.25	11.5	30	7.8	1.56	G	66×66	0.174	963	23	Y	0.63	1.91
	MD-1C-F99S	0.25	11.5	30	7.8	1.56	G	99×99	0.116	586	23	Y	0.63	1.97
[38]	B2A-N-1	0.25	11.5	30	4.66	1.21	G	66×66	0.174	797	25	Y	0.47	1.87
	R4D-N-1	0.40	1.45	35	4.6	1.20	G	66×66	0.174	797	25	Y	0.36	1.84
	R4D-M-1	0.40	1.45	35	7.3	1.51	G	66×66	0.174	797	25	Y	0.36	1.93
	R7E-M-1	0.70	1.45	35	7.3	1.51	G	66×66	0.174	797	25	Y	0.36	1.78
	R7E-Z-1	0.70	1.45	35	11.6	1.91	G	66×66	0.174	797	25	Y	0.36	1.64
	CA-M-1	0.40	1.27	35	7.3	1.51	G	66×66	0.174	797	25	Y	0.18	3.18
[54]	CB_H_M1_s1	0.25	5.35	15	14.5	2.13	H	20×20	0.350	202	6.7	Y	0.30	2.80
	T_G_M1_s1	0.25	3.3	15	14.5	2.13	G	120×120	0.235	960	48	Y	0.25	2.60
	T_G_M2_s1	0.25	3.3	40	6.4	1.42	G	120×120	0.235	960	48	Y	0.25	2.92
	T_H_M1_s1	0.25	3.3	15	14.5	2.13	H	20×20	0.350	202	6.7	Y	0.25	2.24
[55]	37-R2	0.25	6.1	30	0.8	0.50	G	66×66	0.152	600	38	N	0.23	1.60
	39-C	0.25	6.1	30	2.7	0.92	G	66×66	0.152	600	38	N	0.23	2.12
[47]	WG2	0.15	3.5	10	40	3.54	G	30×30	0.090	1280	32	N	0.50	2.48
	WG5	0.15	3.5	10	40	3.54	G	30×30	0.090	1280	32	N	0.50	2.44
[48]	W2-G-11	0.20	3.6	10	40	3.54	G	30×30	0.090	1280	32	N	0.27	3.07
[58]	CRM_M15_SP3	0.25	5.83	30	15	2.17	G	38×38	0.087	1825	25	N	0.40	2.68
[57]	CRM	0.12	8.7	30	9.1	1.69	G	33×33	0.108	1489	48	N	0.53	2.60
[37]	G20	0.23	4.9	12	15	2.17	G	30×30	0.056	1350	33	N	1.03	1.27

[a] Masonry wall specimen: t_w: thickness; $f_{c,URM}$: compressive strength of unreinforced masonry.

[b] CRM system: t_m: overall thickness; f_{cm}: compressive strength of mortar matrix; f_{tm}: tensile strength of mortar matrix computed (in absence of specific information) as 0.56 $f_{cm}^{0.5}$ according to Ref. [51]; Fib.: fibres of the mesh: G: glass, H: hemp; GS: grid spacing of the mesh; t_f: dry fibres of the mesh; f_f: tensile strength of the mesh; E_f: tensile modulus of elasticity of the mesh; TC: transversal connectors: Y: yes; N: no. All specimens were strengthened with CRM applied to both wall sides.

to Ref. [60]). The database was cleaned by applying a set of methodological criteria aimed at ensuring the consistency, comparability, and reliability of the experimental evidence. Only tests performed on masonry panels subjected to in-plane shear were retained, and the experimental setup was required to be compatible with the ASTM diagonal compression procedure [41] or with equivalent configurations capable of producing comparable shear mechanisms. Studies were excluded when essential mechanical or geometric data were missing, when failure modes could not be clearly attributed to shear, or when the strengthening system did not fall within the CRM family as defined in this study. Results affected by evident experimental anomalies, non-representative boundary conditions, or unclear material characterization were also discarded to avoid bias. Lastly, only tests providing measurable shear strength values for both unstrengthened UR and strengthened configurations were retained, ensuring that the contribution of the CRM system was clearly identifiable and could be reliably extracted and compared across the dataset.

The cleaned dataset includes key performance metrics from multiple test campaigns, covering both historic and modern masonry specimens subjected to diagonal compression and shear-compression tests. Reported parameters include wall geometry, masonry type, mortar composition, mesh material and configuration, anchorage details, peak shear loads, and displacement capacities. Comparative results between unstrengthened and CRM-strengthened panels are also provided by the ratio between the average shear stress (computed according to Ref. [41]) attained at collapse by the retrofitted specimen and that of the unreinforced masonry (τ/τ_0), highlighting the improvements in load-bearing capacity.

Overall, the experimental shear strength is closely related to the properties of the applied CRM strengthening system. In particular, it increases with the tensile strength (Fig. 4a) and compressive strength (Fig. 4b) of the mortar matrix overlay (the two are clearly correlated), as well as with the tensile strength of the FRP mesh (Fig. 4c). Strengthening configurations that include anchorage devices generally exhibit higher shear resistance than those without them. On the other hand, the presence of connectors does not affect the correlation between the shear strength and the mechanical properties of the mortar matrix.

3.3. Analytical models

Diagonal compression tests are essential for determining the shear response of CRM-strengthened masonry panels. Nonetheless, they do not capture the full range of mechanisms that may develop in real structural elements. When masonry piers or spandrels are tested under combined shear-axial loading [43,61], or when cantilever-type boundary conditions are considered [52], the strengthening system contributes not only to shear resistance but also to the in-plane flexural capacity, particularly when the reinforcement is adequately anchored. In shear-compression tests, as well as on spandrel elements, CRM overlays have been observed to promote a mixed-mode response. As lateral loads increase, diagonal cracking associated with shear typically coexists with flexural cracking at the element edges, where tensile stresses tend to concentrate. In some cases, the ultimate collapse is governed by shear, while in others, the failure shifts toward a flexural or flexural-compression mode. In this context, the contribution of the mesh is crucial, as once the mortar matrix has cracked, the mesh provides the tensile capacity needed to bridge cracks, stabilize the post-peak response, and prevent sudden loss of load-carrying capacity. This behaviour cannot be inferred from diagonal compression tests alone, yet it is essential for understanding the global seismic performance of strengthened masonry walls. The analytical correlations discussed in this study should therefore be interpreted with their intended purpose in mind, namely, predicting the peak shear strength measured in diagonal compression tests.

The design-oriented models proposed for the pure in-plane shear strengthening of masonry walls with CRM have been adapted from those provided by existing guidelines for reinforced plaster [16] or FRCM systems [17]. To this aim, empirical coefficients have been recalibrated or introduced using available experimental data. However, relying on FRCM-based models to predict CRM behaviour presents some limitations, due to differences between the two systems in terms of material composition, mechanical interaction, and failure mechanisms. Because of the reduced thickness (8-10 mm), the contribution of FRCM systems depends strongly on the bond

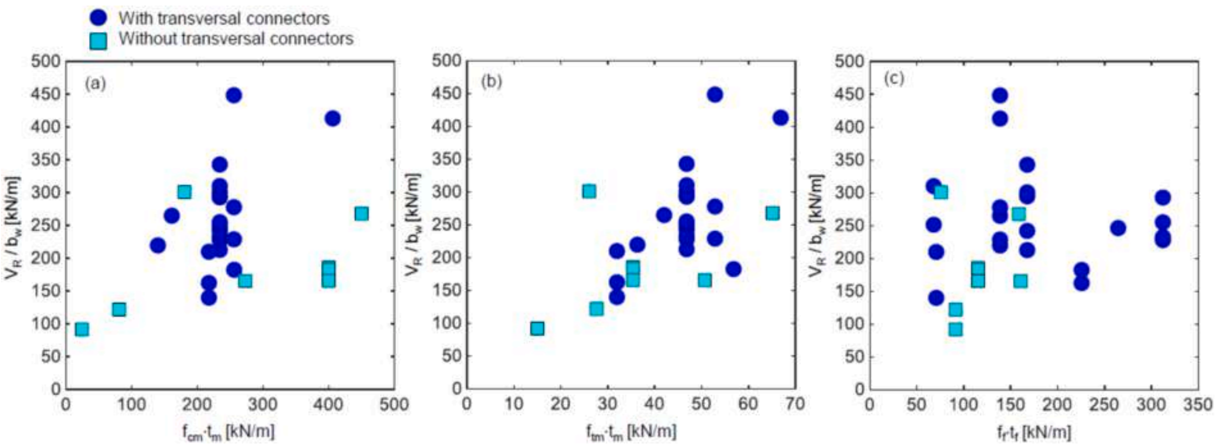

Fig. 4. Correlation between the experimental shear strength of masonry walls strengthened with CRM and the compressive strength of the mortar matrix layer (a), the tensile strength of the mortar matrix layer (b), and the tensile strength of the FRP mesh (c).

behaviour (between textile and matrix and between matrix and substrate) and on the ability of the textile to bridge cracks once the matrix has cracked. In contrast, CRM systems, which use a thicker structural mortar layer (30-40 mm), the role played by the matrix and associated with its mechanical properties and cross-sectional area is stronger, while bond failure is prevented by mechanical connectors, such as the tensile failure of the mesh, which is often attained.

An FRCM-based model generally assumes limited composite action and localized debonding between reinforcement and matrix. These assumptions underestimate the continuous stress transfer that occurs in CRM overlays. If this holds in general for any application, it plays a particularly remarkable role in the case of shear strengthening, as it results in an underestimation of the shear strength or a misrepresentation of the stress distribution within the strengthened wall. In FRCM formulations, the reinforcement contribution is typically expressed as a function of the effective fibre strain and fibre area, with the mortar contribution often considered negligible after cracking. In CRM systems, however, the mortar matrix itself provides a significant portion of the shear and compressive strength, and its interaction with the mesh creates synergistic effects that are not captured by fibre-based models alone. Therefore, applying FRCM formulations directly can lead to an underestimation of the mechanical contribution of the mortar and an omission of the composite action between mesh and mortar that enhances stiffness and energy dissipation. Furthermore, when FRCM-based equations are extended to CRM systems merely by introducing empirical coefficients, their accuracy becomes highly dependent on the calibration database. Because experimental data for CRM systems are still limited and vary across materials (lime vs. cement mortars, glass vs. carbon meshes), the predictive capability of the model may be valid only for the specific conditions used in calibration. This restricts its applicability to different masonry typologies, wall geometries, or boundary conditions.

Nonetheless, a common starting point used in codes and models exists and is the additive approach, meaning that the total shear strength of the retrofitted wall (V_R) is obtained as the sum of the contribution of the unstrengthened masonry (including shear friction and any compression-dependent shear capacity, V_{UR}) and that of the strengthening system (V_r) (Eq. (1)).

$$V_R = V_{UR} + V_r \tag{1}$$

A typical expression for the unstrengthened masonry term may be written as in Eq. (2), in which t_w is the wall thickness, h is the shear length (height of panel), and τ_0 is the shear strength of the unstrengthened masonry, which may depend on the vertical compressive stress (σ_v), cohesion (c), and internal friction φ (e.g., $\tau_0 = c + \sigma_v \tan\varphi$ or an empirical $\tau_0(\sigma_v)$).

$$V_{UR} = t_w\, h\, \tau_0 \tag{2}$$

In FRCM-based models, the contribution of the reinforcement (V_r^{FRCM}) is typically derived from the tensile strength of the textile mobilized across cracks, and is projected into a shear contribution through geometric considerations and an efficiency factor (Eq. (3)):

$$V_r^{FRCM} = k_e\, A_f\, f_{fe}\, \sin\alpha \tag{3}$$

where A_f is the reinforcement area per unit wall width oriented to resist shear, f_{fe} is the effective tensile stress in the fibres under working conditions, α is the angle between the reinforcement tensile direction and the horizontal shear plane (commonly taken as 45°), and k_e is an empirical efficiency factor accounting for bond-slip, load distribution, and partial exploitation of fibre strength, as discussed below.

A more detailed expression developed for FRCM explicitly uses an effective strain $\varepsilon_{f,eff}$ (Eq. (4)):

$$V_r^{FRCM} = A_f\, E_f\, \varepsilon_{f,eff}\, \sin\alpha \tag{4}$$

with $\varepsilon_{f,eff}$ (l_b,τ_b); where E_f is the tensile modulus of elasticity of the textile embedded in the FRCM composite, l_b is the shear bond transfer length, and τ_b is a bond stress parameter. In practice, $\varepsilon_{f,eff}$ is obtained from simplified bond-slip laws and/or experimental calibration [17]. These FRCM-based formulations, as said before, rely on the assumptions that the reinforcement contribution is dominated by the fibres after matrix cracking, fibre strain is governed by bond-slip, the mortar layer is thin, so it contributes negligibly after cracking, and its own compressive or frictional contribution is negligible.

As a first attempt, the approach developed for FRCM could be extended to CRM; indeed, some authors have followed this direction in their formulations. Meriggi and co-authors [62] proposed a design-oriented approach to estimate the shear strength increase provided by externally bonded FRCM and CRM (V_r), to be added to the shear strength of the unstrengthened masonry (V_{UR}) to compute that of the retrofitted wall (V_R). The method assumes that the main contribution arises from the development of a strut-and-tie resisting mechanism, defined on the basis of the mechanical and geometrical characteristics of the FRCM or CRM system. Other contributions, such as the increase in resisting cross-section (compressed diagonal strut provided by the mortar matrix) or the confinement effect ensured by transversal connectors, when present, are neglected in order to derive simplified expressions suitable for engineering practice. The analytical expression for V_r (Eqs. (5) and (6)) was validated experimentally and calibrated according to the design-by-testing procedure of Annex D of Eurocode 0 [30]. Specific coefficients were introduced to amplify the bond capacity (f_b) associated with intermediate debonding ($\alpha_1 = 1.15$), to reduce the tensile strength of the textile (f_t) to account for uneven stress distributions ($\alpha_2 = 1.25$), and to consider the effects of eccentricity in unsymmetrical reinforcements ($\eta = 0.7$ in case of single-side reinforcements). Model uncertainties for ultimate limit state verifications were also considered using a fractile coefficient $\gamma_K = 0.5$ for the calculation of the design strength of the retrofitted wall (Eq. (7)). The authors adopted the assumptions commonly used for FRCM composites and demonstrated that a specific calibration for CRM provides good agreement between experimental results and theoretical predictions.

$$V_r = \eta\ A_f f_f \tag{5}$$

$$f_f = \min\left(\alpha_1 f_b; \frac{f_t}{\alpha_2}\right) \tag{6}$$

$$V_R = V_{UR} + \gamma_k V_r \tag{7}$$

Apart from Ref. [62], the other authors who proposed analytical models specifically for CRM reinforcements introduced additional terms to explicitly and separately account for the contributions of the mortar and of the reinforcement mesh, which will be referred to as V_f and V_{mat} hereinafter, and calibrated them on experimental basis to quantify also the effect of their interactions. These interactions may lead to delayed matrix cracking, increased shear transfer at the masonry-overlay interface (in turn promoted by the mechanical connectors), and a more realistic exploitation of the ultimate capacity of the constituent materials under real-world conditions.

In the early stages of research on this topic, Gattesco and Boem [38,63] proposed a preliminary approach to quantify the shear strength of masonry panels strengthened with CRM, expressed as the sum of the contributions of the unstrengthened masonry and the mortar coating (assumed proportional to its tensile strength), neglecting any contribution from the embedded mesh. Comparison with the strengths obtained from diagonal compression tests (investigating different masonry types and coating mortars) indicated that the predictions were generally on the safe side; therefore, an amplification coefficient $\beta > 1$ was calibrated to improve the accuracy of the estimates, likely accounting for the beneficial influence of the mesh. However, in some cases (e.g., strong and regular masonry with very brittle post-peak behaviour combined with high-strength mortars), the estimates proved unsafe, requiring the calibration of a reduction coefficient $\beta < 1$. In fact, once the brittle masonry cracked, its contribution was suddenly lost, while the contribution of the mortar had not yet been fully mobilized. The authors generally concluded that the different contributors to the shear strength, i.e., the masonry, the mortar coating, and the mesh, need to be considered. However, since they are not mobilized simultaneously, their combination should account for their nonlinear behaviour.

A first model for estimating the total shear strength of the retrofitted wall, going beyond the first uncracked stage, was proposed by Cascardi and co-authors [64]. The model computes the shear resistance of the retrofitted wall (V_R) as a combination of the contributions associated with the unstrengthened masonry (which depends on its compressive strength f_{cUR}, its cross-sectional net area A_{mas}, and a coefficient α accounting for the multi-crack behaviour induced by the presence of the retrofitting), the mesh (V_f) and the matrix (V_{mat}) as shown in Eq. (8) and makes use of the tuning coefficients α, ν, β and γ provided in Eqs. (9)–(12), which were calibrated using artificial neural networks (ANN). The contributions of the mesh (V_f) and of the matrix (V_{mat}) are provided by Eqs. (13) and (14).

In Eqs. (8)–(14), f_{cm} is the compressive strength of the matrix, ε_f and E_f are the tensile strain and modulus of elasticity of the mesh, n is the number of wall sides reinforced with CRM, and n_f is the number of mesh plies per side. The calibration was based a dataset comprising 75 experimental results from diagonal compression tests on masonry panels, encompassing a range of material properties and geometries, and including both FRCM and CRM systems. The ANN approach was selected for its ability to capture complex, nonlinear relationships between input variables and output responses, making it particularly suitable for representing the behaviour of CRM-strengthened masonry walls.

$$V_R = \alpha\ f_{cUR}^{0.5}\ A_{mas} + V_f + V_{mat} \tag{8}$$

$$\alpha = \frac{0.363}{1 + e^{-\nu}} \tag{9}$$

$$\nu = -0.52 + 1.36\beta + 0.05\gamma \tag{10}$$

$$\beta = \frac{n\ n_f\ A_f\ \varepsilon_f\ E_f}{0.7\sqrt{f_{c,UR}}\ A_{mas}} \tag{11}$$

$$\gamma = \frac{f_{cm}}{f_{c,UR}} \tag{12}$$

$$V_f = 0.67\ \ n\ n_f\ A_f\ 0.5\ \varepsilon_f\ E_f \tag{13}$$

$$V_{mat} = 0.1\ n\ A_{mat}\ f_{cm}^{0.5} \tag{14}$$

The model proposed by D'Antino and co-authors [50] extended the approach provided by ASTM 519 [41] to the case of CRM-strengthened square walls by considering only the tensile strength (f_{tm}, herein computed as 0.56 $f_{cm}^{0.5}$ according to Ref. [65]) and the thickness (t_{mat}) of the mortar matrix, and the number of mesh plies per side (n_f) to calculate the contribution of CRM to V_R (Eq. (15)). In this latter expression, b_w and t_w are the wall width and thickness, and f_{tUR} s the tensile strength of UR masonry. The calibration of the analytical model was specifically tailored to CRM systems and was based on diagonal compression tests conducted on masonry walls constructed with historic bricks and strengthened using CRM, focusing on parameters such as wall dimensions, typology (double-leaf with or without diaphragm), and the presence of steel anchors.

$$V_R = \frac{b_w}{0.707}\left(f_{tUR}\ t_w + f_{tm}\ n_f\ t_{mat}\right) \tag{15}$$

The analytical model developed by Thomoglou and co-authors [66] provides an estimate of the shear strength of masonry walls externally strengthened with mortar-based composites, including CRM. The authors proposed a design-oriented approach that accounts for both material and structural parameters, introducing an empirical coefficient (k) to quantify the combined contribution of the mortar and the reinforcement textile/mesh fabric to the overall shear capacity of the strengthened wall (V_R) as expressed by Eq. (16), where V_{UR} is the shear strength of the unstrengthened masonry, and the contributions of the mesh (V_f) and the mortar matrix (V_{mat}) are calculated with Eqs. (17) and (18), in which E_{cm} is the Young's modulus of the matrix and the other symbols are as above.

$$V_R = V_{UR} + k(V_f + V_{mat}) \tag{16}$$

$$V_f = n\, n_f\, A_f\, \varepsilon_f\, E_f \tag{17}$$

$$V_{mat} = n\, A_{mat}\, E_{cm}\, \varepsilon_{mat} \tag{18}$$

The coefficient k of Eq. (16) ranges from 0.52 to 0.60 depending on the masonry unit and reinforcement type, and accounts for the mortar-mesh interaction, which reduces the effective contribution of the CRM system. The authors noted that including the mortar contribution improves the predictive accuracy of the model compared with older formulations that neglected it. However, applying $k < 1$ to both the mesh and matrix terms may underestimate the actual participation of the mortar, which experimental results have shown can reach its tensile strength at the shear capacity of the strengthened masonry.

Similar to Ref. [50], Angiolilli and co-authors in Ref. [65] extended an analytical model originally proposed for three-leaf masonry walls to the case of CRM-strengthened masonry. In this case, the contribution provided by CRM to the shear strength of the wall, V_R, depends on the interaction between the unstrengthened masonry and the mortar of the strengthening overlay and introduces a model coefficient $\lambda_b > 1$, as shown in Eq. (19), in which A_{mas} is the cross-sectional net area of the UR masonry, t_w is its thickness and τ_0 is its shear strength, while A_{mat} and t_m refer to the cross-sectional net area and thickness of the CRM matrix per side, and f_{tm} is the tensile strength of the matrix, determined as a function of its compressive strength f_{cm} as per Eq. (20).

$$V_R = \lambda_b \left(\frac{A_{mas}\, \tau_0\, t_w}{t_w + t_m} + \frac{A_{mat}\, f_{tm}\, t_m}{t_w + t_m} \right) \tag{19}$$

$$f_{tm} = 0.56\, f_{cm}^{0.5} \tag{20}$$

The model proposed in Ref. [65] was developed and calibrated on the basis of cyclic diagonal compression tests carried out on stone masonry specimens extracted from the walls of a historic building in L'Aquila, Italy, considered representative of existing constructions typical of the central Apennines region. The CRM system adopted in the study consisted of a GFRP mesh embedded in a natural hydraulic lime-based mortar, applied as a coating on the masonry surfaces, together with CFRP connectors. The experimental results showed that the application of CRM enhanced the shear strength and the energy-dissipation capacity of the masonry walls, confirming its effectiveness as a strengthening solution for historic structures. It should be noted that the authors proposed to neglect entirely the contribution of the mesh in their analytical model.

In [67], an analytical formulation was proposed to evaluate the shear strength of masonry panels strengthened with FRCM systems, which considers both the contributions of the reinforcing fibres and of the matrix. Although the proposal was developed for FRCM systems, pre-impregnated mesh was considered in the calibration; therefore, the model is herein applied to the CRM scope. The authors observed that the increase in shear strength depends primarily on the expected tensile contribution of the fibres and on the bond strength between the strengthening system and the masonry substrate. Experimental results showed that the attainment of the shear strength generally does not correspond to fibre rupture, highlighting instead the crucial role of the mortar matrix. The analytical model (Eq. (21)) proposes a weighted sum of the contributions from the unstrengthened masonry (V_{UR}), the matrix (V_{mat}), and the mesh (V_f). V_{mat} depends on the number of reinforced wall sides (n), the cross-sectional net area, and the tensile strength of the mortar matrix (f_{tm}) (Eq. (22)). V_f depends on the number of reinforced wall sides (n), the mesh plies per side (n_f), and the area (A_f), ultimate strain (ε_f), and tensile modulus of elasticity of the mesh (E_f), according to Eq. (23), in which the coefficient $\sqrt{2}/2$ accounts for the inclination of the fibres with respect to the principal tensile stress direction.

$$V_R = \alpha_1\, V_{UR} + \alpha_2\, V_{mat} + \alpha_3\, V_f \tag{21}$$

$$V_{mat} = n\, A_{mat}\, f_{tm} \tag{22}$$

$$V_f = \frac{\sqrt{2}}{2}\, n\, n_f\, A_f\, \varepsilon_f\, E_f \tag{23}$$

The empirical coefficients α_1, α_2, and α_3, ranging between 0 and 1, were calibrated on the results of diagonal compression tests and represent the interaction between the CRM overlays and the masonry substrate, depending on the substrate and mesh type. Reported values of α_1 vary between 0.43 and 0.51 for panels strengthened with basalt fabric, corresponding to α_2 values of 0.09-0.10 and α_3 values between 0.75 and 0.91. In general, α_1 can be assumed as 20% of the ratio between the residual capacity of the UR at the second peak of the response curve (the one associated with the tensile failure of the mesh) and its ultimate capacity, while α_2 is approximately 20% of α_1, to reflect the marginal contribution of the mortar. Suggested values for α_3 are 0.63, 0.43, and 0.73 for basalt, carbon, and glass fabrics, respectively.

Longo and co-authors [68] proposed an analytical model for masonry walls strengthened with mortar-based composites (FRCM, CRM, SRG), in which the shear strength of the retrofitted wall is given by the sum of the shear strength of the unstrengthened masonry (V_{UR}) and the contribution provided by the reinforcement (V_r), according to Eq. (24). V_r is calculated as a function of V_{UR} (Eq. (25)) using the coefficients η_f (Eq. (26)) and η_{mat} (Eq. (27)), which represent the geometrical percentages of the mesh and the matrix within the strengthening system, respectively, and were proposed based on a novel design-oriented approach that accounts for the mesh-to-matrix interaction through multiple linear regression.

$$V_R = V_{UR} + V_r \tag{24}$$

$$V_r = V_{UR}\left(0.07\ \eta_f + 1.08\ \ \eta_{mat} - 0.04\ \eta_{mat}^2\right) \tag{25}$$

$$\eta_f = \frac{n\ n_f\ t_f\ \varepsilon_f\ E_f}{t_w\ \tau_0} \tag{26}$$

$$\eta_{mat} = \frac{n\ \ t_m\ 0.56\ f_{cm}^{0.5}}{t_w\ \tau_0} \tag{27}$$

Lastly, Calò and co-authors [60] proposed an analytical model that computes the shear strength of the retrofitted wall (V_R, Eq. (28)) as the sum of the contributions of the unstrengthened masonry (V_{UR}), the matrix (V_{mat}, Eq. (29)), and the mesh (V_f, Eq. (30)). In this latter expression, ψ is the exploitation factor, which quantifies the effective utilization of the tensile capacity of the reinforcement and is defined as the ratio between the effective tensile force developed in the reinforcement and its ultimate tensile capacity. It is calculated as per Eq. (31), with coefficients provided by Eqs. (32)–(34). The exploitation factor accounts for the real-world performance of the reinforcement, recognizing that not all of its theoretical tensile strength is mobilized under service loads due to factors such as imperfect bond, material heterogeneity, and the presence of defects. For the systems studied, ψ is influenced by the interaction between the mortar matrix and the fibre grid, as well as the quality of the bond between these components.

$$V_R = V_{UR} + V_{mat} + V_f \text{ with } \frac{\tau}{\tau_0} \leq 3 \tag{28}$$

$$V_{mat} = n\ A_{mat}\ 0.56\ f_{cm}^{0.5} \tag{29}$$

$$V_f = 0.5\ n\ n_f\ A_f\ \psi\ \varepsilon_f\ E_f \tag{30}$$

$$0 \leq \psi = \frac{e^{\alpha\left(\frac{\eta_{mat}}{\eta_f}\right)} - e^{-\alpha\left(\frac{\eta_{mat}}{\eta_f}\right)}}{e^{\alpha\left(\frac{\eta_{mat}}{\eta_f}\right)} + e^{-\alpha\left(\frac{\eta_{mat}}{\eta_f}\right)}} < 1 \text{ with } \frac{\eta_{mat}}{\eta_f} \leq 0.7 \text{ and } \eta_f > 0 \tag{31}$$

$$\alpha = \alpha_I + \alpha_C + \alpha_S \tag{32}$$

$$\eta_{mat} = \frac{n\ t_m\ 0.56\ f_{cm}^{0.5}}{t_{UR}\ \tau_0} \tag{33}$$

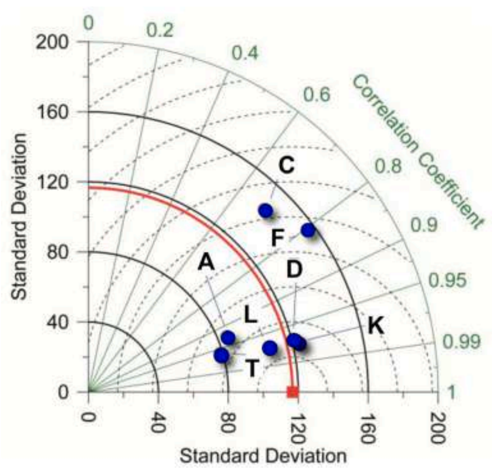

	A	C	D	F	K	L	T
Mean	0.639	1.120	0.924	1.160	1.107	1.010	0.695
St. Dev.	0.151	0.430	0.145	0.392	0.146	0.161	0.114
Median	0.635	1.017	0.935	1.131	1.091	0.983	0.675
Corr. Coeff.	0.862	0.482	0.938	0.649	0.945	0.942	0.921
RMSE	100.7	90.2	32.9	101.7	35.3	29.3	90.2

Fig. 5. Taylor's diagram for the comparison between experimental results of in-plane shear tests and theoretical estimates of the shear strength of masonry walls strengthened with CRM.

$$\eta_f = \frac{n\, n_f\, t_f\, \varepsilon_f\, E_f}{t_w\, \tau_0} \tag{34}$$

The capability of the analytical models described above to estimate the shear strength of CRM retrofitted walls is quantitatively evaluated through direct comparison with the experimental data (averaging consistent results and setting all the design-oriented coefficients to 1) reported in Table 1 using statistical indicators, including standard deviation, root mean square error (RMSE), and the coefficient of determination (R^2), which collectively characterize the agreement between predicted and observed values in terms of accuracy, precision, and linear correlation, respectively. To facilitate the visual interpretation of model performance, Fig. 5 shows a Taylor's diagram [69]. This graphical tool enables the simultaneous representation of correlation, variability, and error magnitude within a polar coordinate system. The red square marker identifies the experimental benchmark, whereas each analytical model is represented by a distinct blue circle, and its position depends on statistical indicators computed from the corresponding array of ratios between theoretical and experimental values; each array contains as many elements as the number of experiments available in the database. The radial axis of the diagram corresponds to one plus the standard deviation, while the angular displacement reflects the correlation coefficient, with angles ranging from 0° to 90° representing R^2 values from 1 to 0, respectively. Concentric circles centred at the reference point denote increasing RMSE values, allowing a compact visualization of model fidelity.

The proximity of a model marker to the reference point directly indicates its predictive accuracy and consistency. The theoretical models are identified in the plot with labels C [64], D [50], T [66], A [65], F [67], L [68], and K [60].

Among the evaluated models, those proposed by Refs. [50], [68], and [60] demonstrated superior performance, exhibiting the most favourable combination of precision, low error, and strong linear correlation with the experimental dataset. These findings reinforce the conclusion that, in the context of CRM strengthening of masonry walls, the dominant structural contribution arises from the mortar layer. Conversely, the influence of the FRP mesh appears secondary and can be either attenuated through calibration or omitted from predictive formulations without significant loss of accuracy.

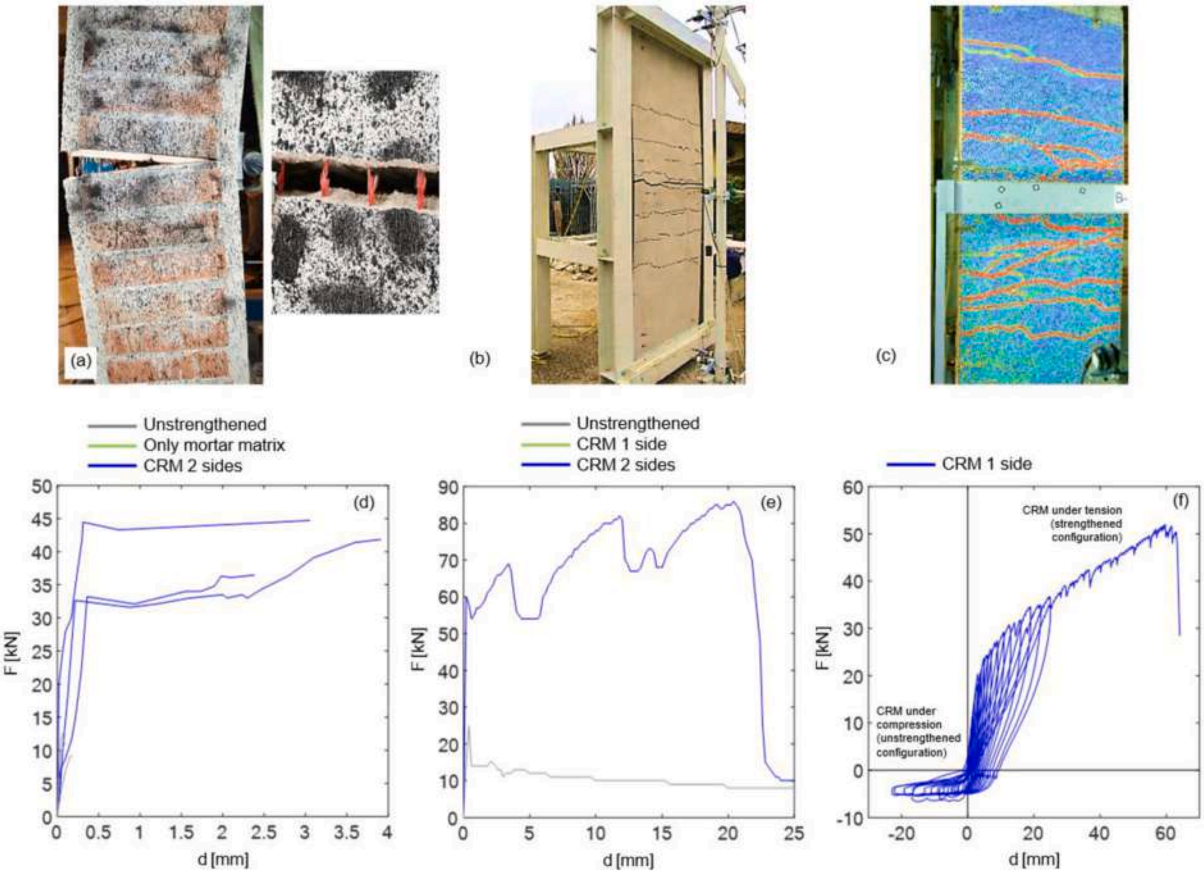

Fig. 6. Crack patterns (a-c), highlighted by DIC strain fields when available (c) and response curves (d-f) of masonry walls strengthened with CRM subjected to out-of-plane bending tests conducted by Ref. [71] (a,d) [72], (b,e), and [42,73] (c,f).

4. Out-of-plane strengthening of masonry walls

4.1. General considerations

Traditional masonry buildings subjected to seismic actions frequently experience the activation of out-of-plane collapse mechanisms [70]. This vulnerability is typically associated with slender walls, weak or missing wall-to-floor connections, flexible diaphragms, or large inter-story heights. However, an additional and equally significant condition occurs in the presence of masonry vaults. During an earthquake, vaulted systems can amplify their lateral thrust, which is transmitted to the adjoining vertical walls. When these walls exhibit low transverse stiffness, the increased horizontal thrust may trigger or accelerate an out-of-plane collapse mechanism. In such configurations, the seismic response is governed not only by the geometry and connections of the vertical walls but also by the dynamic interaction between the vault and the supporting wall system.

Out-of-plane bending induces tensile stresses in the masonry, which inherently possesses low tensile strength, thus triggering a collapse mechanism characterized by mutual rocking among masonry blocks that resist only in compression and whose equilibrium is governed by gravitational loads. The seismic vulnerability to out-of-plane actions is further exacerbated in masonry with very weak mortar, small units, and irregular arrangement, which tends to disaggregate, and in multiple-leaf masonry with unconnected leaves, which tends to exhibit leaf separation, even before the activation of a proper mechanism involving masonry blocks. Experimental studies have demonstrated that applying fibre reinforced composite materials (including CRM systems) on masonry surfaces is an effective strategy to prevent out-of-plane collapses. Their primary contribution lies in their excellent tensile properties, which compensate for the intrinsic weakness of masonry in tension, thereby inhibiting or delaying the activation of collapse mechanisms. The effectiveness of the strengthening system also relies on the adoption of transverse connection devices, such as artificial through elements (sometimes referred to as *diatones*), steel ties, or other suitable connectors, to provide adequate confinement and prevent leaf separation and/or masonry disaggregation.

Under optimal conditions, the out-of-plane failure of a masonry wall strengthened with externally bonded composite reinforcements occurs when the fibres reach their maximum tensile strain. Nevertheless, depending on the geometric and mechanical characteristics of both masonry and reinforcement, as well as on the loading and boundary conditions, premature failure may occur due to debonding or delamination of the composite, crushing of masonry in compressed zones, or shear failure across the wall thickness. The analytical capacity models available in the literature generally account for these possible failure modes. CRM systems, thanks to the high stress transfer capacity provided by the mechanical connectors, that prevents debonding, can enable fibre rupture to be often achieved at failure. Moreover, since such anchors are always present, CRM is inherently effective in enhancing the transversal connection between wall leaves when installed on both sides.

Table 2
Summary of the experimental results of out-of-plane bending tests on masonry walls.

Ref.	Masonry wall specimen [a]					CRM system			Results				Label [f]
	NS [m]	b_w [m]	t_w [m]	Masonry type	Loading scheme [b]	Matrix [c]	GFRP mesh [d]	Config. [e]	F_{max} [kN]	d_u [mm]	ΔF_{max} [−]	Δd_u [−]	
[72]	2.84	1.00	0.25	Brickwork	4P-M	Lime-cement	66mm × 66 mm	UR	9.6	0.38	-	-	
				Single leaf		mortar $t_m = 30$ mm	$t_f = 57.6\ mm^2/m$	R-2	45.5	32.6	4.7	85.8	A
			0.40	Rubblestone		$f_{cm} = 6.3$ MPa	$f_f = 1345$ MPa	UR	25.5	0.46	-	-	
				Double leaf		$f_{tm} = 1.1$ MPa	$E_f = 73.7$ GPa	R-2	86.2	19.9	3.4	43.3	B
			0.40	Cobblestone		$E_{cm} = 14.4$ GPa	L-shaped connectors +	UR	15.1	0.56	-	-	
				Double leaf			artificial diatones for	R-2	101.3[g]	13.8	6.7	24.6	C
[42, 73]	2.70	1.00	0.25	Brickwork	3P-C	Lime-cement	double-leaf walls	UR	3.4	4.3	-	-	
				Single leaf		mortar $t_m = 30$ mm		R-1	35.1	58.6	10.3	13.6	D
			0.25	Brickwork		$f_{cm} = 15.3$ MPa		UR	3.3	23.1	-	-	
				Double leaf		$f_{fm} = 3.4$ MPa		R-1	29.0	44.5	8.8	1.9	E
			0.35	Rubblestone		$E_{cm} = 10.1$ GPa		UR	6.5	2.8	-	-	
				Double leaf				R-1	52.0	63.0	8.0	22.5	F
[71]	1.13	0.80	0.25	Brickwork	3P-M	Lime-cement	27mm × 27 mm	UR	11.1	1.8	-	-	
				Single leaf		mortar $t_m = 30$ mm	$t_f = 29.2\ mm^2/m$	R-2	41.0	5.4	3.7	3.0	G
			0.25	Tuff		$f_{cm} = 8.4$ MPa	$f_f = 1319$ MPa	UR	1.5	0.1	-	-	
				Single leaf		$f_{fm} = 3.0$ MPa	$E_f = 67.0$ GPa	R-2	40.9	3.1	27.3	31.0	H
						$E_{cm} = 12.3$ GPa	Stainless-steel helical conn.						

[a] Masonry wall specimens: NS: net span; b_w: width; t_w: thickness.
[b] Loading scheme: 4P-M: vertical four-point bending tests, monotonic quasi-static loading; 3P-C: vertical three point bending tests, quasi-static cyclic loading; 3P-M: vertical three-point bending tests, monotonic quasi-static loading.
[c] CRM mortar matrix: t_m: overall thickness; f_{cm}: compressive strength; f_{tm}: tensile strength; f_{fm}: flexural tensile strength; E_{cm}: Young' modulus.
[d] GFRP mesh: t_f: dry fibres; f_f: tensile strength; E_f: tensile modulus of elasticity.
[e] Configuration: UR: unstrengthened masonry: R-1: CRM strengthened masonry on one side; R-2: CRM strengthened masonry on two sides.
[f] Label used in the bar chart of Fig. 7b.
[g] Ultimate strength reported to be higher than expected due to friction in the experimental setup.

4.2. Experimental evidence

Several studies available in the literature have investigated the out-of-plane behaviour of masonry walls strengthened with externally bonded mortar-based composites. These studies have employed a wide range of experimental setups and loading conditions, including three- or four-point bending tests, air-bag tests, uniformly distributed loading, eccentric compression, and bi-dimensional bending, as well as different testing procedures such as monotonic, loading-unloading, cyclic, and dynamic protocols (Fig. 6). Variations also exist in the arrangement of the wall prototypes (horizontal or vertical), the bending direction (perpendicular or parallel to the bed joints), and the application of pre-loading through additional axial compression. Most of the existing research has focused on FRCM (see, among others, [74–76]), while comparatively fewer studies have addressed the behaviour of masonry specimens strengthened with CRM [42,71–73,77].

A first experimental investigation was conducted by Ref. [72] and involved monotonic four-point bending tests on full-scale vertically arranged masonry wall specimens (1.0m × 3.0m) with free rotation at both the top and bottom supports (net span of NS = 2.84m) (Fig. 6b). Only the self-weight was considered in the vertical direction. Three masonry typologies were investigated, namely single-leaf solid brickwork (wall thickness $t_w = 0.25$ mm), rubblestone masonry ($t_w = 0.40$m), and cobblestone masonry ($t_w = 0.40$m). For each typology, one specimen was tested in the unstrengthened condition and another was strengthened with CRM on both sides. The CRM consisted of a $t_m = 30$ mm thick hydraulic lime and cement-based mortar ($f_{cm} = 6.3$ MPa compressive strength, $f_{tm} = 1.1$ MPa tensile strength, $E_{cm} = 14.4$ GPa Young's modulus) embedding 66mm × 66 mm GFRP mesh (equivalent to $t_f = 57.6$ mm^2/m of dry fibres, having $f_f = 1345$ MPa tensile strength, and $E_f = 73.7$ GPa tensile modulus of elasticity) and L-shaped GFRP transversal connectors (6/m^2).

The response curve shown in Fig. 6e, with displacement d on the x-axis and horizontal load F on the y-axis, highlights that the CRM strengthening provided a significant increase not only in flexural strength but also in out-of-plane displacement capacity. More specifically, the strengthened specimens exhibited out-of-plane load capacities 3.4 to 6.7 times higher than those of the unstrengthened walls and reached ultimate deflections ranging from 1/206 to 1/87 of the net span prior to collapse. In the unstrengthened specimens, the formation of a single horizontal crack led to the onset of a kinematic mechanism, after which only residual resistance due to self-weight remained. Conversely, in the strengthened specimens, two distinct behavioural stages were identified, such as an initial phase up to the first cracking of the mortar coating, followed by a second phase characterized by the sequential formation of multiple horizontal cracks in the central region of the wall experiencing tensile stresses, accompanied by further strength gains with increasing deflection. Final failure occurred when the vertical glass fibres of the GFRP mesh reached their ultimate strain nearly simultaneously along one of the major cracks.

A second experimental investigation, conducted by the same research group, utilized a CRM system very similar to that already used in Ref. [72], which featured the same 66mm × 66 mm GFRP mesh and L-shaped GFRP transversal connectors (6/m^2), but a different lime and cement-based mortar ($f_{cm} = 15.3$ MPa compressive strength, $f_{fm} = 3.4$ MPa flexural tensile strength, $E_{cm} = 10.1$ GPa Young's modulus). In this occasion, the CRM system was applied on a single side of the masonry only [42,73]. Vertical three-point cyclic bending tests were performed on full-scale masonry specimens (1.0m × 2.5m) equipped with two 0.25m thick reinforced concrete beams at the extremities (NS = 2.7m), with free rotation at the top and bottom (Fig. 6c). Only the self-weight was considered in the vertical direction.

The response curve, represented in the F-d plane as in the previous case, illustrates in the positive quadrant the mechanical behaviour of the specimen under the loading condition in which the CRM system is subjected to tension, thereby contributing to the flexural response of the strengthened wall. In the negative quadrant, the response corresponding to the opposite loading condition is shown, in which the CRM system is located on the compressed side of the wall and therefore does not provide a significant contribution

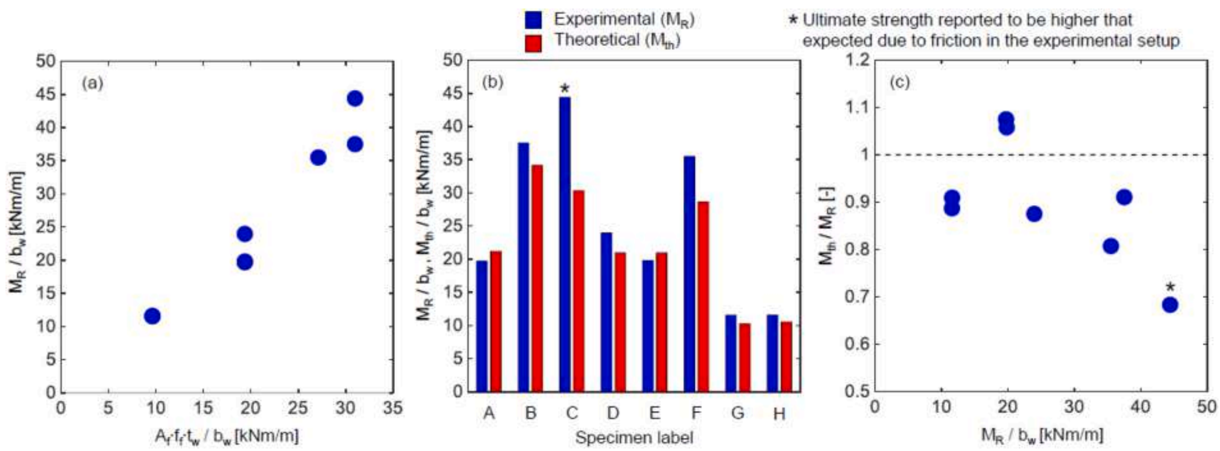

Fig. 7. Out-of-plane bending tests on masonry walls strengthened with CRM: correlation between the experimental resisting bending moment and the strengthening layout (a), comparison between experimental results and theoretical estimates of the resisting bending moment (b), and correlation between accuracy of theoretical estimates and experimental resisting bending moment (c). Tests conducted by Refs. [42,71–73].

to the mechanical behaviour. The comparison between the two quadrants highlights that the strengthening system plays a crucial role in enhancing both the maximum resisting bending moment and the out-of-plane displacement capacity, even under repeated loading cycles.

Three configurations were examined, such as single- and double-leaf brickwork ($t_w = 0.25$m) and double-leaf rubblestone masonry ($t_w = 0.35$m). In the double-leaf specimens, GFRP transversal connectors (4/m^2) were combined with artificial *diatones* (2/m^2), consisting of stainless-steel bars embedded in concrete cores drilled into the masonry. Out-of-plane loading cycles were applied with increasing displacement amplitudes, in both the positive and negative directions; the CRM layer was therefore subjected to tensile (positive loading direction) or compressive (negative) stresses. Once a net deflection equal to 1/150 of the span was reached, the test continued monotonically in the positive direction only. The comparison between the responses in the two loading directions allowed an indicative assessment of the behaviour of strengthened versus unstrengthened masonry, since the contribution of the CRM in compression is negligible apart from the small additional thickness of the mortar layer. This is highlighted by the response curve in Fig. 6f, represented in the F-d plane as in the previous case. The plot shows in the positive quadrant the mechanical behaviour of the specimen under the loading condition in which the CRM system is subjected to tension, thereby contributing to the flexural response of the strengthened wall, and, in the negative quadrant, the response corresponding to the opposite loading condition is shown, in which the CRM system is located on the compressed side of the wall and therefore does not provide a significant contribution to the mechanical behaviour.

Consistently with previous findings [42], negative loading (CRM in compression) led to the formation of one or two sub-horizontal cracks and activation of the collapse mechanism. Conversely, positive loading (CRM under tensile stresses) triggered multiple horizontal cracks spreading from the mid-height region of the specimen, and collapse occurred due to tensile rupture of the vertical bundles of the GFRP mesh. Remarkable strength increases were observed, ranging from 8.0 to 10.3 times, with ultimate deflection values between 1/58 and 1/41 of the span. Lastly, it is worth noting that, in all the tests, no detachment of the CRM layer was observed. This outcome is consistent with the use of mechanical connectors, which are an essential component of the system and proved effective in preventing debonding of the composite overlay from the masonry substrate.

Donnini and co-authors [71] carried out monotonic three-point vertical bending tests on single-leaf brickwork and tuff masonry panels with overall dimensions of 0.8×1.2m (NS = 1.13m) and $t_w = 0.25$m thickness, subjected only to self-weight (Fig. 6a). For each masonry type, three specimens were tested in the unstrengthened condition, followed by three additional specimens strengthened with a CRM system applied on both faces. The CRM consisted of a $t_m = 30$ mm thick layer of hydraulic lime and cement mortar, ($f_{cm} = 8.4$ MPa, $f_{fm} = 3.0$ MPa, $E_{cm} = 12.3$ GPa) embedding a 27mm × 27 mm GFRP mesh ($t_f = 29.2$ mm^2/m, $f_f = 1319$ MPa, $E_f = 67.0$ GPa), and supplemented with transverse stainless-steel helical connectors.

Unstrengthened panels failed after the formation of a single horizontal crack in the midspan region. In the strengthened specimens, once the mortar layer had cracked, the embedded mesh remained intact and continued to carry load, producing a substantial increase in both resistance and deformation capacity until failure occurred due to tensile rupture of the vertical mesh yarns at the horizontal crack location (Fig. 6a). The bending capacity increased on average by approximately 3.7 times for brickwork and 27.3 times for tuff masonry, with corresponding ultimate deflections of about 1/209 and 1/365 of the span, respectively. Consistently with the experimental findings commented above, no detachment of the CRM layer was observed. This outcome is attributable to the mechanical connectors, which effectively ensured load transfer between the CRM overlay and the masonry substrate, preventing debonding phenomena.

The response curves shown in Fig. 6d illustrate the differences in terms of flexural strength and out-of-plane displacement capacity between CRM-retrofitted specimens and unstrengthened ones. Moreover, the comparison with the response curves discussed above (Fig. 6e and f), irrespective of the load and deflection values that cannot be directly compared, highlights that the experimental outcomes are strongly dependent on the adopted test setups, boundary conditions, and the presence of axial load. In particular, it can be observed that the ability to sustain both loads and displacements under repeated loading-unloading cycles can be more effectively investigated when tests are performed on large-scale specimens and under combined bending and axial compression conditions. Naturally, these represent more complex and costly experimental conditions; however, they are likely better able to replicate the

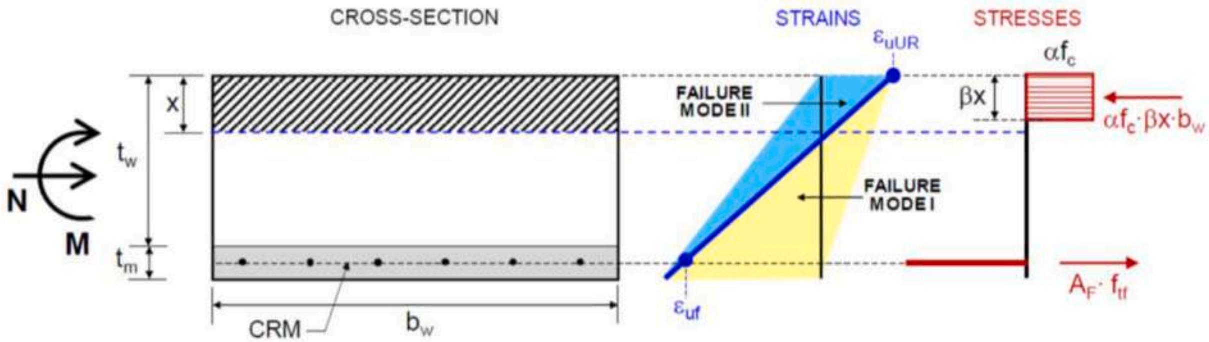

Fig. 8. Cross-section of a masonry wall strengthened with CRM, and strain and stress profiles, for calculating the resisting bending moment under the hypothesis of tensile rupture of the fibres, with compressive strains in the plateau. Neutral axis position at balanced failure.

boundary and loading conditions experienced by structural elements within an actual building.

Table 2 summarizes the results of the experimental investigations described above, reporting the maximum applied force F_{max} and the corresponding ultimate deflection d_u. The table also provides the strength and deformation increments ΔF_{max} and Δd_u, calculated as the ratio between the strengthened and the unstrengthened configurations. Lastly, although the number of experimental tests available in the scientific literature is relatively limited, the outcomes indicate a correlation between the resisting bending moment and the strengthening configuration, in particular with the tensile strength of the FRP mesh and the wall thickness (Fig. 7a).

4.3. Analytical models

According to the scientific literature [72,78] and existing technical guidelines [16–18], the flexural capacity of a masonry wall strengthened with mortar-based composites (i.e., the maximum resisting bending moment, M_R) can be estimated through a cross-sectional analysis. This capacity primarily depends on the mechanical properties of the masonry and the composite, the thickness of the masonry panel, the boundary conditions, and the axial compressive stress. Theoretical models have been primarily developed for FRCM composites, and in absence of specific alternatives, they can also be considered for CRM-reinforced walls. Such models adopt the classical beam theory assumptions for reinforced sections subjected to combined axial load and bending, namely: (i) plane sections remain plane, (ii) perfect bond exists between CRM and masonry (thanks to the proper installation of a certain number of transversal connectors per square metre according to the manufacturer provisions), (iii) the masonry constitutive relationships in compression are assumed to be linear-plastic (or parabolic-plastic) up to ultimate strain (typically $\varepsilon_{uUR} = 0.35\%$), while the tensile contribution is neglected, and (iv) the tensile behaviour of the CRM is linear-elastic up to the attainment of its limit strain (ε_{uf}), while the contribution of CRM under compression is neglected.

The resisting bending moment is calculated from the rotational equilibrium equation, and the neutral axis in the cross-section from the axial equilibrium equation (Fig. 8). Different cases are distinguished, and the solution is the lowest of the three, namely crushing at the compressive edge with the fibres in the tensile elastic range (Failure mode I), or attainment of the limit tensile strain of the fibres, with either compressive strain in the plateau or a linear stress distribution in compression (Failure mode II). In the cited studies, the collapse always occurred for the tensile rupture of the fibres with the compressive strain in the plateau, thus Eq. (35) applies.

$$M_R = \alpha f_c b_w \beta x \left(\frac{t_w + t_m}{2} - \beta \frac{x}{2}\right) + A_F f_{tf} \left(\frac{t_w + t_m}{2} - \frac{t_m}{2}\right) \tag{35}$$

In Eq. (35), b_w is the width of the masonry cross-section, t_w and t_m are the thickness of the masonry and of the CRM layer, f_c is the compressive strength of masonry, $\alpha = 0.85$ and $\beta = 0.70$ are the stress block coefficients, A_F and f_{tf} are the cross-sectional area and the tensile strength of the CRM reinforcement (i.e., of its FRP mesh), N is the compressive axial force, and x is the depth of the neutral axis, provided by Eq. (36).

$$x = \frac{N + A_F f_{tf}}{\alpha f_c b_w \beta} \tag{35a}$$

Notably, this behaviour differs from FRCM systems, where typically, the composite-to-substrate load transfer relies on adhesion and failure may occur due to debonding, such that the limit strain, or the maximum stress, are associated to debonding and not to the tensile rupture of the fibres, as in the case of CRM.

The resisting bending moments of the masonry wall specimens strengthened with CRM described above were analytically evaluated by applying Eq. (35) (mean mechanical properties were considered), to assess the reliability of the analytical model. The results are reported in Fig. 7b showing that, although neglecting the compressive contribution of the mortar, the model approximates with good accuracy the experimental results. A larger dataset would be needed to develop more robust conclusions; however, the comparison between analytical predictions and experimental results suggests that the analytical methods tend to underestimate the actual load-carrying capacity observed in the tested specimens, particularly for large-scale walls, which exhibited higher flexural strength (Fig. 7c). However, this is likely related to the adopted CRM strength values (f_{tm}), obtained from tests on single wires and thus neglecting the beneficial group effect of multiple mesh wires, as well as the stress homogenizing effect of the mortar matrix.

5. Crowning beams

5.1. General considerations

Reinforced masonry crowning beams (also referred to as ring beams) can be constructed at the top of walls or, more rarely, at floor levels to enhance their out-of-plane bending capacity and to ensure an effective connection between orthogonal walls, thereby providing the structure with a box-type behaviour and an adequate transfer of actions during earthquakes. These crowning beams are typically constructed using rubble stone or clay bricks, depending on the existing masonry, which yields good compatibility with this latter, in terms of mass and stiffness. An effective connection must, of course, be ensured using vertical mechanical connectors. Crowning beams may be strengthened with steel or composite bars. The use of the FRP meshes developed for CRM systems has also been investigated for this application. The meshes are embedded within the bed joints during the construction of the crowning beam, with appropriate overlaps at the intersections between orthogonal walls.

Table 3
Results of bending tests on masonry crowning beams and theoretical estimates.

Ref.	Crowning beam specimen [a]					FRP mesh [b]					Results [c]		Label [d]
	h [m]	b [m]	f_c [MPa]	Masonry type	Test dir.	Type	t_f [mm^2/m]	f_f [MPa]	E_f [GPa]	n_f [−]	M_R [kNm]	M_{th} [kNm]	
[79]	0.09	0.50	11	FT	O	GFRP	110	1252	77.4	3	19.0	23.4	A
	0.09	0.80	11	SM	I	33mm × 33 mm	110	1252	77.4	3	3.7	5.6	B
[80]	0.50	0.50	3.4	SM	I	GFRP	97	840.1	85.3	3	22.7	29.0	C
	0.50	0.50	3.4	SM	O	12mm × 12 mm	97	840.1	85.3	3	17.4	24.1	D
	0.50	0.50	3.4	SM	I	+ PBO cords	97	1483.6	150.7	4	24.2	47.0	E
	0.50	0.50	3.4	SM	O		97	1483.6	150.7	4	22.7	39.1	F
	0.50	0.50	3.4	SM	I	GFRP	160	1252	77.4	4	50.5	41.8	G
	0.50	0.50	3.4	SM	O	33mm × 33 mm	160	1252	77.4	4	44.3	34.0	H
	0.50	0.50	3.4	SM	I		160	1252	77.4	4	54.7	41.8	I
	0.50	0.50	3.4	SM	O		160	1252	77.4	4	40.8	34.0	J
	0.30	0.40	11	HB	I		160	1252	77.4	5	39.7	28.0	K
	0.30	0.40	11	HB	O		160	1252	77.4	5	30.7	33.0	L
[81]	0.66	0.35	2.5	SM	O	GFRP	57.6	1345	72.8	4	14.0	12.9	M
	0.47	0.25	6.7	SB	O	66mm × 66 mm	57.6	1345	72.8	6	9.3	8.4	N

[a] Masonry crowning beam specimen: h: height; b: width; f_c: masonry compressive strength; masonry type: FT: solid flat tiles; SM: stone masonry; SB; solid bricks; HB; hollow bricks; Test dir.: test direction: O: out-of-plane; I: in -plane.

[b] FRP mesh: t_f: dry fibres; f_f: tensile strength; E_f: tensile modulus of elasticity; n_f: number of mortar joints embedding the mesh.

[c] Results: M_R: resisting bending moment from experimental tests; M_{th}: resisting bending moment from theoretical model.

[d] Label used in the bar chart of Fig. 9b.

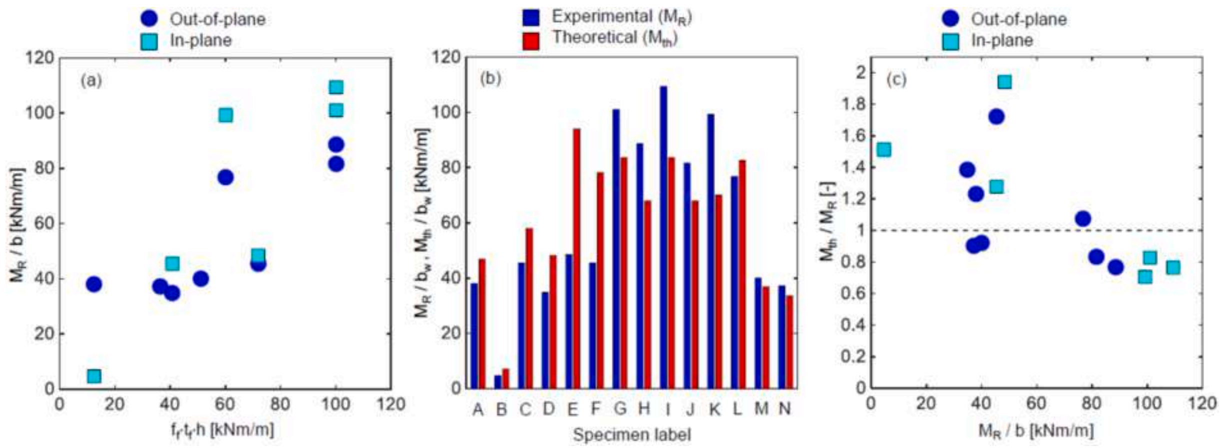

Fig. 9. Bending tests on crowning beams reinforced with FRP meshes: correlation between the experimental resisting bending moment and the tensile strength of the FRP mesh and the strengthening layout (a), comparison between experimental results and theoretical estimates of the resisting bending moment (b), and correlation between accuracy of theoretical estimates and experimental resisting bending moment (c). Tests conducted by Refs. [79–81].

5.2. Experimental evidence

Few experimental investigations [79–81] have explored the possibility of constructing masonry crowning beams by placing the FRP meshes of CRM within the bed joints, to provide tensile and bending strength. In the first work [79] ring beams built with solid flat tiles were reinforced by embedding 33mm × 33 mm GFRP mesh ($t_f = 110\ mm^2/m$, $f_f = 1252$ MPa, $E_f = 77.4$ GPa) in the bed joints; one specimen was tested under out-of-plane loads (bending axis orthogonal to the bed joints) and another one under in-plane loads

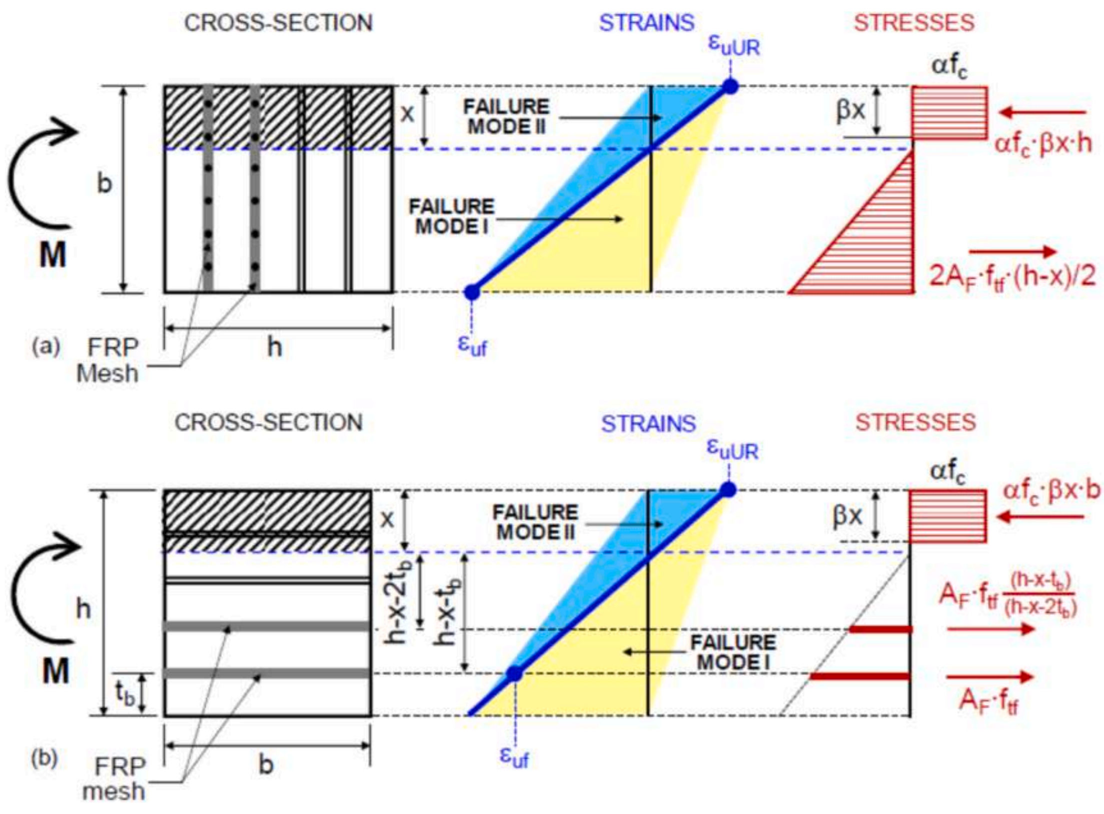

Fig. 10. Cross-section of a masonry crowning beam reinforced with FRP mesh in two bed joints, and strain and stress profiles, under horizontal bending (out-of-plane loads, a) and vertical bending (in-plane loads, b), for calculating the resisting bending moment under the hypothesis of tensile rupture of the fibres. Neutral axis position at balanced failure.

(bending axis parallel to the bed joints). Bending tests were conducted on simply supported beams with 3.80m net span with a four-point bending scheme using a hydraulic actuator.

In the second study [80], crowning beam specimens were built with stone masonry and with hollow bricks and reinforced in the bed joints with different meshes. Two meshes were composed of 12mm × 12 mm GFRP sheets and PBO cords ($t_f = 97$ mm^2/m, $f_f = 840$ MPa, $E_f = 85.3$ GPa for twisted cord configuration; $t_f = 97$ mm^2/m, $f_f = 1483$ MPa, $E_f = 150.7$ GPa for unidirectional cord configuration) and one mesh was the same 33mm × 33 mm GFRP mesh used in Ref. [79]. Also in this case, bending tests were conducted on simply supported beams with 4.00m span, but the load was applied by means of concrete blocks and mortar bags.

The third experimental campaign [81] concerned masonry crowning beams with a length of 3.5m, having 66mm × 66 mm GFRP meshes ($t_f = 57.6$ mm^2/m, $f_f = 1345$ MPa, $E_f = 72.8$ GPa) embedded in the bed joints and tested under horizontal cyclic loading. Two different masonry types were considered: rubble stones (beam cross section 350mm × 660 mm, total of 4 strengthened bed joints) and single wythe solid bricks (250mm × 465 mm, total of 6 strengthened bed joints). The horizontal translations at the two lateral ends of the specimen were restrained, while the beam lay on trolleys allowing free horizontal deflection (net span 3.0m). An actuator alternating pushed and pulled the samples midspan, with progressively increasing displacements.

The results of the cited studies, listed in Table 3, demonstrate that FRP meshes can increase load-bearing capacity, improve stress distribution, and allow greater deformations before failure of the masonry crowning beam. Tests indicated that strengthened masonry is less sensitive to local defects and that the continuous reinforcement limits crack propagation, especially under concentrated vertical loads and simulated seismic actions, resulting in a more uniform response. Overall, these experimental outcomes suggest that masonry crowning beams reinforced by FRP meshes constitute a promising technology for enhancing the structural performance of masonry walls while remaining compatible with pre-existing structural members in terms of mass and stiffness. Although limited in number, the experimental results highlight a correlation between the experimental resisting bending moment and the CRM strengthening layout, specifically showing an increase in flexural capacity with higher tensile strength of the FRP mesh and greater height of the crowning beam (Fig. 9). However, the tests also showed that the effectiveness of the intervention is compromised if the reinforcement is not properly embedded within the mortar layer.

5.3. Analytical models

The analytical method proposed in the literature, and foreseen in existing design guides for FRCM composites [17,18], to estimate the flexural strength of reinforced masonry crowning beams is based on a cross-sectional analysis under the assumptions of strain compatibility between masonry and mesh and plane section conservation (Fig. 10). The approach is analogous to that adopted for masonry walls subjected to bending, but, in the case of crowning beams, no axial compression acts on the cross-section in this case. The constitutive model for the mesh is linear elastic-brittle in tension, while a stress block diagram is adopted for masonry in compression. The tensile strength of masonry and the compressive strength of the mesh are neglected. Flexural failure of the crowning beam cross-section can occur either through crushing of masonry in compression (mode I) or tensile rupture of the mesh (mode II) and is primarily driven by out-of-plane loads inducing horizontal bending in the crowning beam (Fig. 10).

Horizontal bending is generated by external loads directed out of the plane of the wall (Fig. 10a). In the case of failure for the tensile rupture of the fibres (occurring when their strain equals ε_{uf}, and the corresponding stress equals f_{tf}), which is the most common collapse mode observed in experiments, the resisting moment for out-of-plane bending is provided by Eq. (37), in which b and h are the width and the height of the crowning beam, f_c is the compressive strength of masonry, $\alpha = 0.85$ and $\beta = 0.70$ are the stress block coefficients, f_{tf} is the tensile strength of the FRP mesh, A_F is the cross-sectional area of one mesh layer (it is hereinbelow assumed that the mesh is placed in two bed joints, for the sake of an example), and x is the depth of the neutral axis, determined from the equilibrium of internal forces (Eq. (38)).

$$M_R = 2A_F f_{tf}\left(\frac{h-x}{2}\right)\left(\frac{2}{3}h+\frac{1}{3}x-\frac{1}{2}\beta x\right) \tag{37}$$

$$x = \frac{A_F f_{tf} h}{A_F f_{tf} + \alpha f_c \beta h} \tag{38}$$

Vertical bending is generated by external loads directed in the plane of the wall (Fig. 10b), and is rare, as it would require partial or complete collapse of the underlying wall. In this case, the resisting moment is provided by Eq. (39), assuming, as the sake of an example and as above, that the FRP mesh is placed in two bed joints of the crowning beam, and that failure occurs when the first mesh layer attains its ultimate strain ε_{uf}, which corresponds to a stress equal to the tensile strength f_{tf}.

$$M_R = A_F f_{tf}\left(h - t_b - \frac{1}{2}\beta x\right) + A_F f_{tf}\frac{h-x-t_b}{h-x-2t_b}\left(h-2t_b-\frac{1}{2}\beta x\right) \tag{39}$$

In Eq. (39), t_b denotes the thickness of a single layer of the masonry crowning beam (e.g., the height of one brick), while x is the depth of the neutral axis, determined from equilibrium by solving Eq. (40), where b is the width of the crowning beam, and the other symbols are as above.

$$\alpha f_c \beta b x^2 - \left[\alpha f_c \beta b(h-2t_b) + 2A_F f_{tf}\right]x + A_F f_{tf}(2h-3t_b) = 0 \tag{40}$$

The comparison between analytical predictions and experimental results is presented in Fig. 9b and c. The reliability of the theoretical models is not always fully satisfactory, as they tend to overestimate the load-carrying capacity of thinner crowning beams, while slightly underestimating the capacity, generally within 20-25% error, for higher crowning beams, which exhibit higher resistance. No significant differences in the accuracy of the analytical models are observed between bond beams subjected to in-plane and out-of-plane bending.

Lastly, formulations are also provided for tensile loading, which corresponds to the action of the crowning beam at the corners connecting orthogonal walls, allowing the structure to exhibit a box-type behaviour under horizontal forces. In this case, the tensile capacity of the crowning beam depends solely on the net area of the reinforcing mesh placed in the bed joints and is included in the calculations of local overturning collapse mechanisms.

6. Strengthening of arches and vaults

6.1. General considerations

Arches and vaults are widespread in masonry constructions, especially in historical monuments, as well as in residential buildings and bridges. Curved surfaces make it possible to cover large spans taking advantage of the high compressive strength of masonry. The system performs well under vertical loads, and structural stability is ensured when the thrust line remains within the thickness of the element. The behaviour changes under earthquake-induced horizontal actions or under highly unsymmetric loading conditions. In these cases, a progressive collapse can occur, characterized by the formation of a kinematic mechanism with hinge openings that develop in different patterns depending on the boundary conditions. This explains the growing need for effective and non-invasive strengthening solutions that can prevent or limit the hinge openings that lead to collapse mechanisms. Composite materials can inhibit kinematic failure mechanisms and thereby significantly enhance the structural capacity of curved masonry surfaces, thanks to their tensile strength. CRM systems, in particular, have been tested in several studies for the retrofitting of arches and vaults, where they are mainly tensile-activated in the regions where hinges would typically form in the un-strengthened configuration.

Experimental investigations on CRM-strengthened arches are still limited compared to those conducted on masonry walls, particularly under in-plane loading. Nevertheless, the available studies have demonstrated the potential of CRM for this application. Existing guidelines on mortar-based composites [17,18] provide general recommendations for the strengthening of masonry arches and suggest performing cross-sectional analyses at potential hinge sections for collapse analyses (consistently with the approach described in Section 4). However, the exact position of the hinges is not known a-priori and, besides, the bending resistance of the cross section is influenced by the axial load, in turn depending on the hinge position and on the lateral load amplitude. This interdependency makes the analytical estimation of the arch resistance rather complex (an example of an analytical strategy was proposed by Ref. [82]). The practical implementation of this approach in routine engineering practice is not straightforward, and no applications in the design of CRM-strengthened arches have yet been reported in the literature (although several interventions have already been carried out in practice).

6.2. Experimental evidence

Several recent experimental studies have demonstrated the effectiveness of FRCM composites for the retrofit of masonry arches, highlighting the significant increases in both strength and displacement capacity that can be achieved by bonding the reinforcements either at the intrados or at the extrados [83–88], possibly in combination with the reinforcement of buttress walls [89], and even under dynamic excitations [90]. Conversely, investigations employing CRM systems are far less numerous [91–95].

The first experimental study on CRM-strengthened vaults was conducted by Gattesco and co-authors [91] on barrel masonry vaults with thickness s = 0.12m, span S = 3.98m, radius R = 2.06m, rise r = 1.54m, corresponding to a rise-to-radius ratio (r/R) of 0.75, and, lastly, a width b = 0.77m (Fig. 11a). The specimens, built with solid bricks and thin lime mortar joints, were subjected to quasi-static cyclic horizontal loads applied at sixteen points along the vault sides, simulating the distributed mass and aiming at evaluating the seismic response of the retrofitted vaults. Three configurations were tested, such as one unstrengthened (as reference), one strengthened with a CRM system applied at the extrados, and one with the same system applied at the intrados. The reinforcement consisted of a pre-mixed mortar based on hydraulic lime and cement, having 9.8 MPa compressive strength, 1.7 MPa tensile strength, 10 GPa modulus of elasticity and overall thickness of 30 mm, embedding a GFRP mesh, with 66mm × 66 mm grid spacing, 4.5 kN tensile strength of the longitudinal wire and 25.3 GPa tensile modulus of elasticity, and L-shaped connectors with 7mm × 10 mm

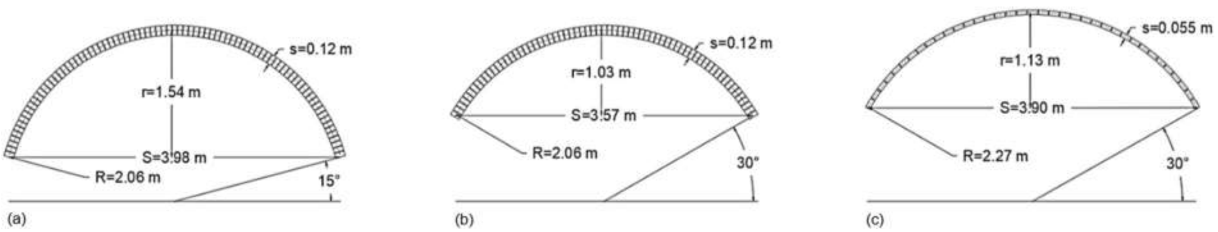

Fig. 11. Masonry vaults tested by Ref. [91] (a) [92], (b), and [93] (c).

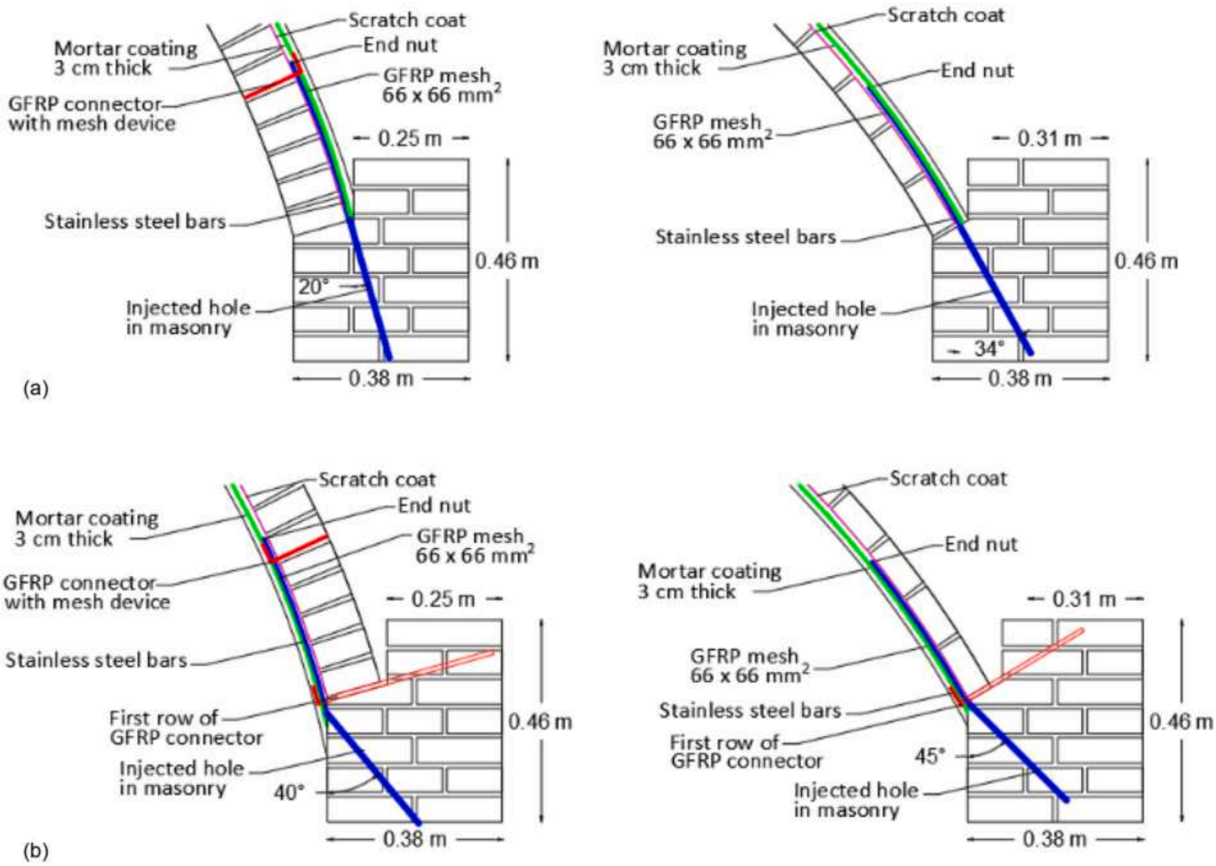

Fig. 12. Connections at the abutments for CRM applied to the intrados (a) and to the extrados (b) of masonry vaults [93].

cross-section and 36 kN tensile strength. The results showed that the CRM strengthening system significantly enhanced the vault capacity in terms of both maximum horizontal load and ultimate displacement. The ultimate load of the strengthened specimens increased by 3.7 and 2.5 for the extrados- and intrados-strengthened configurations, respectively. Furthermore, the retrofitted vaults exhibited larger displacements and improved ductility, which was attributed by the authors to the increased deformation capacity associated with cracking in the matrix and the concentrated rotations occurring at the hinges formed on the unstrengthened side of the vault.

This experimental program was later extended by the same authors through testing three additional vault prototypes, built with the same masonry type and strengthened with a similar system [92]. The vaults had the same thickness ($s = 0.12$m), radius ($R = 2.06$m), and width ($b = 0.77$m) as in the previous study, but different span ($S = 3.575$m) and rise ($r = 1.03$m), corresponding to a rise-to-radius ratio of $r/R = 0.50$ (Fig. 11b). One vault was tested unstrengthened, one was strengthened at the extrados, and one at the intrados. The experimental results confirmed the effectiveness of the CRM, showing that the presence of reinforcement delayed the formation of the final hinge required for the collapse mechanism to develop. Specifically, for vaults of the same geometry, extrados-strengthened specimens achieved significantly higher strength gains, but slightly lower displacement capacities compared to those strengthened at the intrados. Conversely, the larger-span vaults exhibited greater ultimate displacements but lower load-bearing capacities than the smaller ones.

Vault prototypes with a reduced thickness were tested in the investigation presented in Ref. [93], in which the role of the abutments of a mechanical connection between the vault barrel and the side walls was also considered. In this study, two-barrel vaults were constructed using bricks arranged in a running bond pattern, with a thickness of $s = 0.12$m, span $S = 3.98$m, radius $R = 2.06$m, rise $r = 1.545$m ($r/R = 0.75$) and width $b = 0.77$m. Four additional specimens were built using brick in folio masonry, with a thickness of $s = 0.055$m, span $S = 3.90$m, radius $R = 2.27$m, rise $r = 1.155$m ($r/R = 0.50$), and width $b = 0.77$m (Fig. 11c).

To reproduce the presence of the supporting walls, all vaults were built on masonry abutments 0.46m high and 0.77m wide. The CRM reinforcement, which had the same properties of the one adopted in the previous studies, was applied either at the vault extrados or at the intrados. Moreover, in one specimen of in folio masonry vault an additional 15 mm thick mortar layer was interposed between the masonry and the CRM to simulate cases in which removal of the existing plaster is impractical or could damage the vault, making direct overlay application preferable. Three stainless-steel M6 bars were inserted at both skewbacks to prevent sliding in both the transverse and longitudinal directions, as well as uplift (Fig. 12).

Table 4 collects the results of the experimental investigations described above, and lists the maximum vertical load F_{max} and the

Table 4
Summary of the experimental results of tests on masonry vaults.

Ref.	Masonry vault specimen [a]					CRM reinforcement			Results				Label [f]
	R [m]	S [m]	r [m]	s [m]	b [m]	Matrix [b]	GFRP mesh [c]	Configuration [d]	F_{max} [kN]	d_{max} [mm]	ΔF_{max} [−]	Δd_{max} [−]	
[91]	2.06	3.98	1.54	0.12	0.77	Lime-cement mortar $t_m = 30$ mm	66mm × 66 mm $t_f = 7.3$ mm^2/m	UR	3.8	0.8	-	-	A
						$f_{cm} = 9.8$ MPa	$f_f = 4.5$ MPa	R-EX	14.1	76.0	3.7	95	B
						$f_{tm} = 1.7$ MPa	$E_f = 25.3$Gpa	R-IN	11.6	93.0	3.7	116.3	C
						$E_{cm} = 10$Gpa							
[92]	2.06	3.575	1.03	0.12	0.77	Lime-cement mortar $t_m = 30$ mm	66mm × 66 mm $t_f = 7.3$ mm^2/m	UR	13.0	23.0	-	-	D
						$f_{cm} = 9.8$ MPa	$f_f = 4.5$ MPa	R-EX	33.9	49.3	2.6	2.1	E
						$f_{tm} = 1.7$ MPa	$E_f = 25.3$Gpa	R-IN	29.6	59.6	2.3	2.6	F
						$E_{cm} = 10$Gpa							
[93]	2.06	3.98	1.545	0.12	0.77	Lime mortar $t_m = 30$ mm	66mm × 66 mm $t_f = 7.3$ mm^2/m	R-EX + C	22.9	108.1	6.0	135.1	G
						$f_{cm} = 8.6$ MPa	$f_f = 4.5$ MPa	R-IN + C	13.4	130.9	3.5 [e]	163.6 [e]	H
						$f_{tm} = 1.1$ MPa	$E_f = 25.3$Gpa						
						$E_{cm} = 8.5$Gpa							
	2.27	3.90	1.135	0.055	0.77	Lime mortar $t_m = 30$ mm	66mm × 66 mm $t_f = 7.3$ mm^2/m	UR	0.6	1.0	-	-	I
						$f_{cm} = 8.6$ MPa	$f_f = 4.5$ MPa	R-EX + C	11.0	115.5	18.3	115.5	J
						$f_{tm} = 1.1$ MPa	$E_f = 25.3$ GPa	R-IN + C	8.2	105.3	13.7	105.3	K
						$E_{cm} = 8.5$ GPa		R-IN + C + M	13.1	39.0	21.8	39.0	L

[a] Masonry vault specimens: R: radius; S: span; r: rise; s: thickness; b: width.
[b] CRM mortar matrix: t_m: overall thickness; f_{cm}: compressive strength; f_{tm}: tensile strength; E_{cm}: Young' modulus.
[c] GFRP mesh: t_f: dry fibres; f_f: tensile strength; E_f: tensile modulus of elasticity.
[d] Configuration: URM: unstrengthened arch; R-EX: arch unstrengthened with CRM on the extrados; R-IN: arch unstrengthened with CRM on the extrados; +C: additional connectors at the abutments; +M: additional mortar layer.
[e] Calculated with respect to the values of the first row.
[f] Label used in the bar chart of Fig. 13a and b.

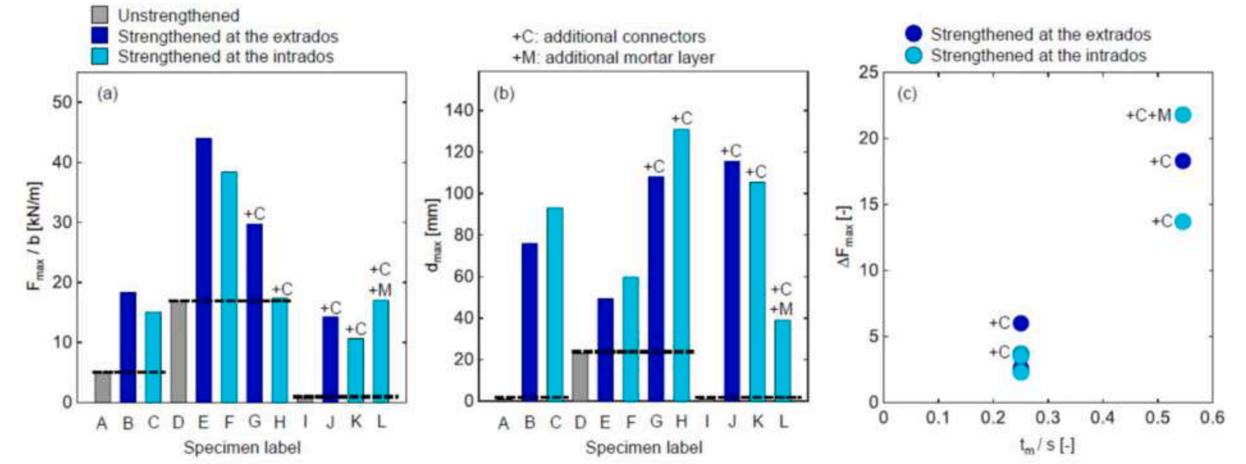

Fig. 13. Tests on masonry arches strengthened with CRM: maximum vertical load (a) and corresponding ultimate displacement (b) and correlation between the maximum load increase and the ratio between CRM and vault thicknesses (c). Tests conducted by Refs. [91–93].

corresponding ultimate displacement d_{max}, together with the strength and deformation increments ΔF_{max} and Δd_{max} calculated as the ratio between the strengthened and the unstrengthened configurations. Experimental results showed that CRM reinforcement applied at the extrados proved more effective than that applied at the intrados (Fig. 13). In both cases, the strengthening led to a significant performance improvement, with ultimate load increases of 4-6 times for vaults built in running bond and even 15-22 times for brick in folio vaults, due to the larger increase of cross-section thickness resulting from CRM application in these very slender specimens.

The vault with an additional mortar layer and intrados reinforcement achieved a 60% higher strength than the corresponding specimen without the layer, owing to the thicker composite section (Fig. 13a). On the other hand, its displacement capacity was lower due to partial detachment of the mortar from the masonry substrate (Fig. 13b). Finally, as concerns the connections, the stainless-steel bars, acting mainly in tension, provided a partial rotational restraint at the skewbacks. Some progressive pull-out of the bars from the mortar was observed; however, no visible uplift occurred at the vault supports.

Fig. 13c shows the correlation between the maximum load increase of the CRM-retrofitted specimens with respect to the unstrengthened ones (ΔF_{max}) and the ratio between CRM mortar (t_m) and vault (s) thicknesses. The limited number of tested specimens available in the scientific literature, together with the restricted variability in terms of strengthening thickness, does not allow any definitive conclusions to be drawn. Therefore, the trend observed in the plot should be interpreted only as a preliminary indication. Nevertheless, it is consistent with previous experimental evidence obtained for other composite strengthening systems, which has shown that the introduction of such reinforcement techniques is particularly effective for highly slender arch elements.

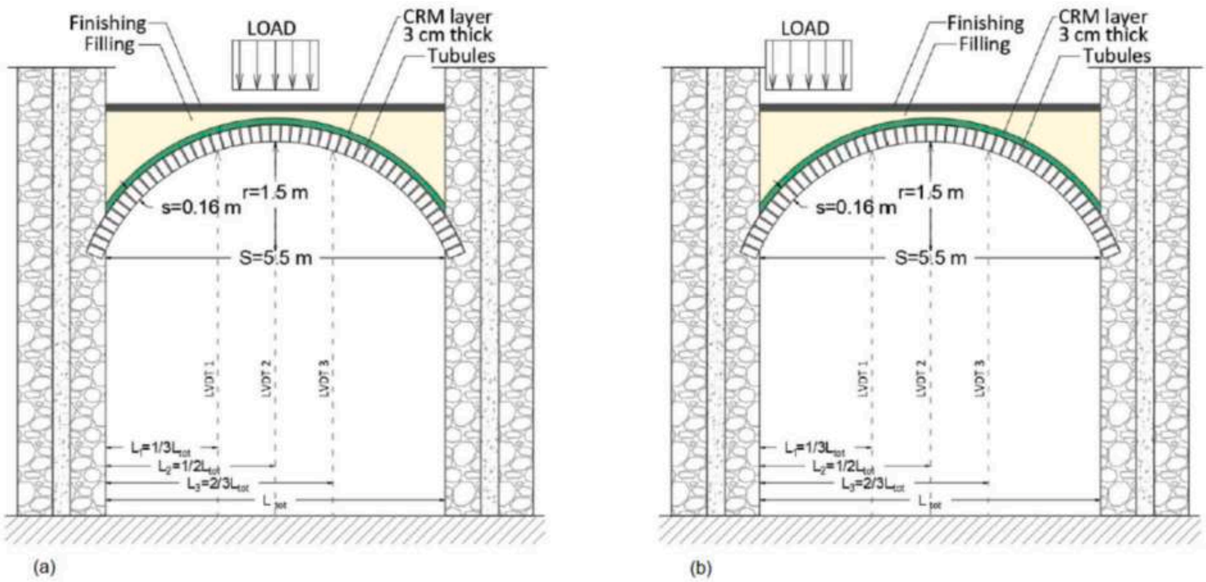

Fig. 14. Masonry vault tested by Ref. [95] under centred (a) and eccentric (b) vertical load.

The experimental results of these investigations were complemented by numerical simulations that enabled a detailed analysis of the influence of different geometric and mechanical parameters on the behaviour of the strengthened vaults [92]. Using the experimentally tested reinforcement system and the measured mechanical properties of the masonry as input data, a numerical model was developed based on a continuum approach combined with a simplified discrete modelling strategy at the springing sections. Nonlinear static analyses were performed, showing a high level of accuracy in reproducing the backbone trend of the experimental capacity curves. Further parametric analyses revealed that increasing the stiffness of the GFRP mesh reduced the vault deflection without significantly affecting its load-carrying capacity, whereas a lower GFRP tensile strength led to premature collapse, with reduced ultimate load and displacement values. Within the examined range of variation (±25%), changes in the mechanical properties of the masonry or the mortar overlay (tensile strength and stiffness) had only a limited effect on the overall performance of the vault. The strengthening efficiency of the CRM system was found to be higher for thinner vaults and for masonry with lower strength and higher self-weight, as well as for vaults with smaller rise-to-radius ratios.

An experimental investigation was carried out in situ by Cascardi and co-authors [95], in which a CRM reinforcement system was applied to a vault made of hollow ceramic tubules bonded with lime-based mortar, a constructive typology that can be found in both historical and modern buildings. The tested structure was a pavilion vault with plan dimensions of 5.5m × 4.7m, thickness $s = 0.16$m (corresponding to the height of the tubules), span $S = 5.5$m, radius $R = 4.0$m, and rise $r = 1.5$m ($r/R = 0.375$).

The CRM system was applied to the extrados of the vault. The mortar matrix was a lime-based mortar with $f_{cm} = 11.3$ MPa, $f_{tm} = 4.0$ MPa, $E_{cm} = 8.1$ GPa, and $t_m = 30$ mm. The GFRP mesh had 66mm × 66 mm grid spacing, $t_f = 3.6$ mm^2/m, $f_f = 485$ MPa, and $E_f = 25.3$ GPa. The CRM systems included steel connectors.

The load was applied along a 1.8m wide, 5.0m long strip on the vault surface (the latter approximately corresponding to the full vault length), using 25 kg cement bags incrementally added to reach a surface load up to 4 kN/m^2. Two loading configurations were considered, such as a centred load and an eccentric load applied at one third of the span (Fig. 14). Linear Variable Displacement Transducers (LVDTs) were placed at strategic locations on the vault to monitor displacements throughout the loading process, with the aim of assessing the variation in structural stiffness associated with the CRM. Under the centred load condition of 4 kN/m^2, the maximum recorded displacements were 0.46 mm (downwards) and 0.12 mm (upwards), while residual deformations were negligible. The vault was not tested prior to reinforcement, so no comparisons could be made with the unstrengthened configuration of the structure. Nonetheless, according to the authors, the measured displacements indicated that the retrofitted vault behaved as a rigid diaphragm under design load levels. Given that ceramic tubule vaults are substantially voided systems, with a much lower solid fraction than conventional masonry, they are known to behave as deformable diaphragms and are typically modelled as such in professional practice, the observed stiffness was attributed to the CRM overlay.

The authors concluded that the full-scale experimental test demonstrated effectiveness of the CRM in significantly increasing the stiffness of the vault. Such an improvement is particularly beneficial under seismic actions, as it enables a more uniform distribution of forces within the structure, reducing stress concentrations that may trigger localized failures. Moreover, the increased stiffness helps limit excessive displacements of the vault, thereby maintaining global stability and preventing collapse. On the other hand, it was not possible to drive the arch to collapse; therefore, no direct information is available regarding the effectiveness of the CRM system in terms of load-carrying capacity enhancement. For this reason, the results of these in-situ tests are not included in Table 4 and Fig. 13.

7. Seismic upgrade

The experimental investigations presented in the previous sections on CRM-strengthened masonry walls subjected to in-plane or out-of-plane loading were primarily aimed at isolating the behaviour of individual structural elements under specific boundary conditions and loading scenarios. These tests, typically quasi-static, simulated seismic effects indirectly by applying cycles of progressively increasing load amplitude. While such quasi-static approaches provide valuable information on element-level response, they cannot capture the fully dynamic effects of earthquake loading, nor the complex interaction mechanisms that govern the seismic behaviour of masonry buildings. In particular, factors such as the interaction between orthogonal walls, the coupling between walls and floors, the thrusts exerted by floor slabs, the presence of openings, and construction details affecting leaf-to-leaf bonding are critical for the development of a global box-type structural response during seismic events.

To address these aspects and gain insight into the dynamic performance of masonry structures, full-scale or large-scale shake table tests are required, ideally subjected to one or multiple seismic input records applied at the base. In this context, two recent experimental investigations were carried out to validate the effectiveness of CRM systems for seismic upgrading of masonry buildings. These studies also aimed at developing low-impact strengthening solutions compatible with conservation requirements and ongoing building use.

De Santis and de Felice [77] investigated the seismic performance of a full-scale tuff masonry structure strengthened using CRM. The prototype consisted of a U-shaped configuration built with 0.25m thick walls, reaching a height of 3.41m and including a façade with a window and a side wall with a door, which introduced asymmetry and structural vulnerability. An inclined timber roof with additional masses was placed on top. The unstrengthened structure exhibited limited seismic capacity, with collapse triggered by the loss of interlocking between the left wall and the façade, driven by out-of-plane demands amplified by the opening.

The adopted CRM system comprised a $t_m = 30$ mm thick composite mortar layer with an alkali-resistant glass-FRP mesh, having 66mm × 66 mm grid spacing, 11.6 mm^2 cross-sectional area of each fibre bundle (corresponding to $t_f = 57.6$ mm^2/m of dry fibres), $f_f = 494$ MPa tensile strength, and $E_f = 25.4$ GPa tensile modulus of elasticity. The matrix was a natural hydraulic lime-based mortar classified as M10 strength class according to Ref. [96]. Mechanical anchorage was provided by L-shaped GFRP connectors (having 10mm × 7 mm cross section) and prefabricated mesh corner elements designed to restore wall-to-wall continuity. Strengthening was applied only to the damaged external surfaces of the left wall and of the façade, leaving the interior undisturbed, an approach consistent with low-impact and conservation-oriented retrofit strategies.

Shake table tests using four natural accelerograms demonstrated a clear improvement in seismic response after CRM strengthening. The base acceleration at collapse increased from approximately 0.41g in the unstrengthened condition to 0.89g after intervention (+120%). When an additional steel tie-bar was later installed at the right corner, the system remained stable up to 1.78g, corresponding to a +335% increase relative to the original capacity. The dynamic response also showed substantial gains in deformability. The out-of-plane displacement capacity of the façade increased by more than 7 times, while in-plane displacements increased by up to nearly 4 times. The CRM strengthening system prevented recurrence of the original failure mechanism; instead, collapse shifted to the unstrengthened right wall, which experienced shear cracking. Overall, the results demonstrated that CRM significantly enhanced both strength and deformation capacity while satisfying low-invasiveness requirements. It was also shown that system can be applied externally within the thickness of a traditional plaster layer, is compatible with historical materials through the use of NHL mortar, and offers a rapid installation process.

The possibility of improving the seismic capacity of masonry walls by applying CRM to only one side has recently been explored also by Gattesco and co-workers [73] through quasi-static tests under in-plane and out-of-plane loading. The test results indicated that one-sided reinforcements are less effective than double-sided ones, due to the reduced amount of strengthening material and, to a lesser extent, to the unsymmetrical effects introduced in the structural member. However, the authors concluded that the maximum load, ultimate displacement, and energy dissipation under cyclic loading were appreciably improved, although the enhancements may be insufficient when substantial increases in structural performance are required.

Another shake table test was conducted by De Santis and co-workers [97] on full-scale fair faced rubble masonry walls strengthened using a low-impact CRM-based system. Also in this case, natural accelerograms were selected as seismic base input. The tested wall was 3.73m high, 0.50m thick, and 1.63m wide, constructed with rubble stone units recovered from collapsed historic buildings and lime-based bedding mortar replicating traditional practice (based on analyses conducted on sampled collected in the field within post-earthquake surveys). The wall was strengthened with a combination of two techniques, adopting a method originally proposed in Ref. [98]. On the fair faced external side, mortar joints were repointed and reinforced with stainless-steel micro-cords, spaced approximately 500 mm in both vertical and horizontal directions, whereas the internal plastered side was strengthened with CRM, making use of a 66mm × 66 mm GFRP mesh (with the same properties of the one used in Ref. [77]) and a $t_m = 30$ mm thick layer of a lime-based mortar developed to provide both a structural strengthening and a thermal insulation. Stain-less steel threaded bars were inserted in transversal drilled holes to provide connection between micro-cords and GFRP mesh and prevent leaf separation.

Shake table tests showed that the strengthening system significantly improved seismic performance. The base acceleration at the onset of damage increased from 0.22g (unstrengthened reference) to 0.58g (+163%), while the maximum base acceleration at collapse rose from 0.45g to 0.99g (+120%), while out-of-plane displacement capacity remained comparable to the unstrengthened specimen. Progressive damage and leaf separation were effectively constrained by the combination of reinforced repointing, stainless-steel cords, and the CRM overlay, delaying masonry disintegration. Multi-input/multi-output dynamic identification analyses were conducted to calculate vibration frequencies and showed that the initial wall stiffness increased by 20%, and that crack propagation and damage accumulation were substantially reduced.

Test outcomes indicated that the proposed strengthening technique not only provided a significant upgrade in seismic capacity, but also provided the additional advantages that the energy efficiency was improved, and the fair-faced aspect of the external façade was preserved, thus ensuring compatibility with original masonry materials and architectural conservation, offering a low-impact, sustainable solution suitable for the rehabilitation of heritage masonry in earthquake-prone areas.

Finally, recent investigations have addressed post-earthquake reconstruction strategies in which CRM-derived meshes are employed as transversal interconnecting elements in multi-leaf masonry walls [99]. In the proposed reconstruction technique, the internal leaf in steel reinforced hollow brick masonry provided the primary load-bearing capacity, whilst the external leaf consisted of fair-face rubblestone, for which externally bonded overlay systems such as FRCM or CRM are generally unsuitable due to architectural compatibility requirements. The connection system was based on a modified CRM-type GFRP mesh, specifically adapted by increasing the grid spacing (132 mm) and reducing stiffness (employing a highly deformable epoxy resin) to improve constructability and accommodate irregular stone geometries. Shake table tests on a full-scale wall prototype confirmed the effectiveness of the connection system in limiting leaf separation and masonry disaggregation. These results indicate that CRM-type meshes can be effectively employed beyond their conventional use in external strengthening layers, functioning instead as mechanical interconnection devices in seismic-resistant multi-leaf masonry structures.

8. Integration of strengthening and energy retrofitting

Recent technological advances in construction materials, particularly in CRM technology and its constituents, together with the increasing cultural and technical awareness of the environmental impact associated with the construction and operation of buildings, have driven the research community toward innovative solutions that integrate structural strengthening with energy retrofitting. In this context, CRM systems specifically developed to simultaneously address both objectives within a unified intervention have attracted growing attention, considering the potentially beneficial features of CRM, which is applied in the form of plastering, preferably to the entire building envelope, or at least large portions of it, with a relevant thickness (≥30 mm). Despite this growing interest, such integrated approaches are still a relatively recent research line, characterised by heterogeneous approaches, limited experimental datasets, and the absence of consolidated design frameworks.

Cleary, the thermal resistance of a CRM layer depends on the thickness and type of the mortar matrix, while the FRP mesh has no role. The main parameter is the thermal conductivity (λ), which is an intrinsic material property measuring its ability to conduct heat, and is measured in W/m•K, where lower values indicate better insulating performance. Accordingly, when a mortar matrix exhibits both sufficient mechanical strength and low thermal conductivity, it becomes suitable for the unified structural and thermal retrofitting. This challenge has attracted the interest of several researchers in recent years.

One of the first studies was conducted by Artino and co-authors [100], who proposed a methodological framework for a Decision Support System (DSS) designed to orient sustainable deep renovation strategies for existing buildings by jointly addressing seismic safety and thermal efficiency. The DSS was organised into sequential phases, including the characterisation of the building and its context, the definition of feasible renovation strategies, the evaluation of seismic and energy performance improvements, and the assessment of sustainability indicators. Emphasis was placed on interoperability between seismic assessment methods and energy performance analyses, ensuring that improvements in one domain do not negatively affect the other, and highlighting the complexity of this issue. A possible solution had already been suggested by the same authors one year earlier [101] for an integrated retrofit strategy for reinforced concrete buildings, addressing both seismic vulnerability and poor energy performance by replacing the external leaf of double-leaf infill walls with high-performance autoclaved aerated concrete (AAC) blocks. From a structural standpoint, the enhanced infill panels provided increased stiffness and strength, resulting in marked improvements in seismic performance. From an energy perspective, AAC blocks significantly reduced the original thermal transmittance.

A unified retrofitting approach for existing masonry that simultaneously addresses poor seismic performance and inadequate thermal comfort was primarily investigated in Refs. [57,102–104]. The authors developed and experimentally assessed a novel geopolymer-based CRM system designed to retrofit masonry walls on both faces, with the dual aim of enhancing in-plane shear strength and reducing thermal conductivity compared with traditional lime-based CRM composites. Their experimental programme on small-scale masonry panels demonstrated that the geopolymer-based system provided mechanical performance comparable to, and in some respects superior to, conventional solutions, particularly in terms of higher ductility under shear loading, and significantly improved thermal resistance due to the reduced conductivity of the mortar.

It should be noted that not all the investigated solutions can be strictly classified as CRM systems, as several studies focussed on multifunctional coatings or modified mortars originally conceived for thermal retrofitting and subsequently assessed for their mechanical contribution. In this framework, Plassiard and co-authors [105] investigated the influence of an innovative multifunctional coating on the in-plane mechanical behaviour of masonry wallets. The study compared uncoated specimens with specimens coated on both faces using either a highly insulating aerogel-based coating or a commercial competitor. Although both coatings were originally intended for thermal refurbishment, their structural contribution was also evaluated. Experimental results showed that uncoated walls failed in a brittle manner with relatively low lateral strength, whereas coated walls exhibited increased shear strength and a markedly more ductile response. The commercial coating yielded the highest strength gain, while both coatings allowed substantially larger displacements at failure, which is advantageous for energy dissipation during seismic events. The authors concluded that even coatings with modest mechanical properties may be effectively adopted to enhance the thermal performance of the building envelope within a dual-efficiency retrofit strategy.

Parcesepe and co-authors [106] experimentally investigated the mechanical and thermal behaviour of hemp-lime mortar as a sustainable retrofitting material combining renewable resources with low environmental impact. The addition of hemp fibres was found to modify the failure mode toward increased ductility, without improving overall mechanical strength, mainly due to inhomogeneous fibre distribution, which increased porosity and slightly weakened the composite. Nevertheless, environmental exposure often led to strength gains due to additional hydration of the hydraulic lime binder. Thermal tests revealed that the inclusion of hemp fibres reduced thermal conductivity by 10%, indicating improved insulation potential even at low fibre contents, thus making this material promising for combined seismic and energy upgrade.

Lastly, the study by Majumder and co-authors [107] provides a review of seismic and thermal retrofitting methods for masonry buildings based on fibre reinforced composites. The review covers a wide range of approaches, including resin-based and mortar-based systems, as well as emerging solutions using natural fibres of animal and plant origin. These materials are discussed in terms of their ability to enhance in-plane strength, ductility, and energy dissipation capacity of masonry walls under lateral loads, while also offering potential thermal benefits through modifications of the wall assembly and insulation properties. Particular attention is devoted to integrated retrofitting techniques in which structural strengthening and thermal insulation are combined in a single intervention, such as CRM applications, reflecting a rapidly growing research trend.

To date, most available studies primarily address either material-level properties or small-scale wall specimens, while comprehensive investigations at the structural scale, as well as unified analytical or design-oriented models capable of jointly accounting for mechanical and thermal performance, remain scarce. Overall, this research field offers highly promising prospects for substantial advances in both scientific investigation and technological development. Progress in this area requires the coordinated contribution of complementary expertise, the systematic collection of experimental evidence across multiple scales, and the development of robust theoretical and design-oriented models to ensure effective transfer into engineering practice, structural rehabilitation.

9. Installation issues

Experimental studies available in the scientific literature on CRM strengthening systems, while primarily focused on assessing their structural effectiveness under different loading conditions and supporting the development and validation of analytical models, also provide a growing body of evidence on construction details and execution aspects that are critical to the reliable performance of these interventions. Although such aspects are often reported as secondary outcomes of experimental campaigns and are derived from a limited number of case studies, they offer valuable qualitative and quantitative indications on installation requirements, detailing solutions, and critical issues that may affect the effectiveness of CRM systems when applied in practice. These indications, which span different structural typologies and strengthening configurations may serve as a starting point for the progressive definition of best practices for the correct execution and workmanship of CRM strengthening interventions aimed at ensuring their effectiveness and, ultimately, the safety of the strengthened masonry elements.

With specific reference to the strengthening of masonry walls, the experimental evidence consistently indicates that the effectiveness of CRM systems is strongly dependent on the achievement of adequate anchorage conditions. Sufficient anchorage length must be provided to prevent excessive slip between the FRP mesh and the mortar matrix, as well as to avoid internal delamination within the composite layer or debonding from the masonry substrate. This aspect is particularly critical in one-sided strengthening applications, where continuity of the CRM overlay at wall extremities plays a key role in maintaining the contribution of the system. An effective connection between the CRM layer and both the foundation system and the floor diaphragms is also essential. Experimental studies suggest that this can be achieved by embedding vertical stainless-steel bars within the mortar overlay, either anchored into the foundation or passing through the floor systems. Pull-out tests may be employed to calibrate the spacing and detailing of these bars, ensuring that their resistance is compatible with that of the CRM system and that premature anchorage failure is avoided.

Lateral continuity of the CRM is likewise important, especially in the presence of out-of-plane horizontal loads. Experimental observations indicate that stress concentrations and premature cracking may develop at wall intersections or corners if continuity is not properly ensured. To mitigate this issue, angular or corner devices made of FRP mesh can be overlapped with the main mesh panels to guarantee an effective transfer of stresses across orthogonal walls. Similar considerations apply to crowning beams or bond beams, for which an effective mechanical connection to the masonry substrate must be ensured, typically through the use of vertical mechanical connectors. Experimental studies report that such elements may be strengthened using either steel or composite bars embedded within the mortar matrix. When crowning beams are realized across the full thickness of the masonry, the FRP mesh should also extend through the entire thickness. At wall intersections or corners, mesh overlap over the full depth of the bond beam is required to ensure continuity in stress transfer between adjacent mesh layers.

As regards vaulted masonry elements, available investigations allow for qualitative considerations that can support practical applications. The experimental evidence indicates that CRM contributes to limiting the formation and opening of hinges that govern typical collapse mechanisms of vaulted structures. Accordingly, the strengthening system should be placed on either the intrados or the extrados surface, depending on the expected tensile stress distribution, in order to counteract hinge opening and enhance both load-carrying and displacement capacity under vertical static and horizontal dynamic actions. When placement on the theoretically optimal surface is not feasible, the choice must be guided by the anticipated collapse mechanism as well as by practical constraints such as accessibility, construction feasibility, and conservation requirements, particularly in the presence of paintings or elements of historical value.

The effectiveness of CRM overlays on vaulted elements depends primarily on the tensile strength of the embedded FRP mesh and on the ability of the system to transfer stresses to the masonry substrate. While bond performance is a critical issue in FRP and FRCM systems, this aspect is less limiting for CRM applications, which inherently rely on mechanical connectors to ensure load transfer between the composite layer and the masonry. As a consequence, although extrados applications are generally preferred for FRP and FRCM systems due to favourable normal stress components that enhance adhesion, this distinction appears to be less pronounced for CRM. In line with this observation, published studies recommend the use of mechanical connectors for both intrados and extrados applications, distributed along the entire vault barrel, with connector densities on the order of six connectors per square metre reported as effective in experimental campaigns.

Additional connectors at the abutments have also been shown to play a crucial role in preventing crack localisation at the interface between the vault and the supporting walls, thereby promoting a more distributed cracking pattern and enhanced energy dissipation. These connections are typically achieved by embedding stainless-steel bars within the CRM matrix. For extrados strengthening, the bars should be anchored into holes drilled into the skewbacks along the arch direction, whereas for intrados applications, holes inclined at approximately 45° to the vertical and passing through the impost plane have been shown to be effective. Furthermore, additional transverse connectors installed in the skewback region are recommended to prevent premature detachment or slippage of the reinforcement layer, as observed in experimental tests. A major limitation associated with the application of CRM systems on large masonry surfaces concerns the labour-intensive and time-consuming installation, involving three main phases: (i) the application of a first layer of mortar on the masonry substrate; (ii) the positioning and light pressing of the FRP mesh onto the fresh mortar layer; and (iii) the application of a second mortar layer to fully embed the mesh within the matrix. When applied to extensive wall surfaces, these operations significantly increase installation time and overall intervention costs, particularly in the presence of irregular substrates or architectural constraints, as the process is largely manual and requires skilled workmanship to ensure correct mesh alignment, adequate mortar compaction, and proper installation of mechanical connectors. Recent studies have explored alternative strategies aimed at reducing installation complexity by spraying the mortar matrix directly onto the FRP mesh, thereby minimizing manual layering operations and significantly accelerating construction times [77], or by resorting to mortars with dispersed short fibres, thus eliminating the need for a continuous mesh [108,109].

Overall, the available evidence clearly indicates that further coordinated efforts within the scientific community, in close interaction with structural designers and manufacturers/suppliers, are required to consolidate the experimental knowledge and translate it into more comprehensive and reliable recommendations for the proper installation and workmanship of CRM strengthening systems. Such efforts are essential to move from preliminary, literature-based indications toward shared and robust guidelines capable of ensuring the effectiveness and safety of CRM strengthening interventions across different structural typologies and practical applications.

10. Conclusions

The state-of-the-art review conducted on Composite Reinforced Mortar (CRM) systems provides a picture of the current level of knowledge, mainly based on experimental evidence, and highlights existing research gaps that still limit a fully rational and design-oriented application of these systems for the strengthening of masonry structures.

10.1. Experimental evidences

The available experimental results clearly demonstrate the effectiveness of CRM systems in enhancing the structural performance of masonry constructions, particularly in terms of load-carrying capacity, stiffness, and ductility. The most extensively investigated application concerns the in-plane shear strengthening of masonry walls through laboratory tests under diagonal compression and combined compression and shear. In this context, a substantial body of experimental work has shown significant increases in shear resistance, improved post-peak behaviour, and enhanced energy dissipation capacity.

Although less numerous, other applications have also produced meaningful and encouraging results. Tests on masonry walls under compression and out-of-plane bending have demonstrated that CRM can effectively delay crack propagation, increase bending resistance, and enhance overall stability. Similarly, experimental investigations on arches indicate a beneficial contribution of CRM in modifying collapse mechanisms and increasing ultimate capacity, even though the number of tested specimens remains limited and further systematic research is required. The construction of reinforced crowning beams using CRM-compatible solutions also represents a promising strategy to improve box-like behaviour and overall structural response.

Beyond conventional strengthening objectives, recent experimental campaigns have explored broader and more integrated applications. These include in-depth seismic performance assessments through shake table tests, the use of single-sided CRM systems for minimally invasive interventions, particularly relevant for architectural heritage, and the integration of structural strengthening with energy retrofitting measures. Such studies highlight the versatility of CRM and its potential role within holistic rehabilitation strategies that address structural safety, conservation requirements, and sustainability targets simultaneously.

Future research should focus on expanding the experimental database for less investigated structural typologies, such as arches and vaulted systems, as well as systematically assessing cyclic, and long-term behaviour. Experimental studies are also needed to determine the optimal number and distribution of transverse connectors to ensure efficient stress transfer and to counter typical failure mechanisms of masonry, especially in historic structures, such as separation between leaves and disintegration of masonry units. The emergence of sustainable reinforcement materials, such as hemp fibres, also represents a promising direction, offering comparable mechanical performance with reduced environmental impact. However, variability in mechanical properties and the influence of matrix composition on fibre behaviour necessitate more rigorous standardization and testing. Similarly, the use of CRM systems in post-fire rehabilitation has opened new avenues for structural recovery, yet the differential performance of various fibre types under thermal exposure calls for targeted research into high-temperature-resistant composites.

10.2. Analytical models

Analytical models specifically calibrated for CRM still present an immature stage of development. Current procedures often rely on simplified methods or on formulations developed for FRP or FRCM, but the direct extension of these approaches to CRM is not always appropriate. CRM systems feature a thicker mortar layer and mechanical connectors that prevent debonding, resulting in distinct stress transfer mechanisms, strain distributions, and, in some cases, modified failure modes. The use of a fully composite FRP mesh, compared to the dry or partially impregnated fabrics of FRCM, also affects mechanical and long-term behaviour, and this has already led to the development of separate protocols for material characterization and certification.

No analytical formulations are available for CRM retrofitted arches. As concerns walls, distinction should be made between flexural and in-plane strengthening. For flexural strengthening, simplified approaches based on sectional bending analysis appear, at least at a preliminary design level, sufficiently adequate. In such cases, the structural behaviour can be reasonably approximated by adopting compatibility of strains and equilibrium of internal forces, with the CRM system contributing as an additional tensile reinforcement layer.

Conversely, in-plane strengthening mechanisms are significantly more complex. Compared to thinner systems such as FRCM, CRM systems introduce a non-negligible increase in wall thickness and a three-dimensional interaction between the mortar layer, fibre mesh, connectors, and masonry substrate. Shear transfer mechanisms involve cracking of the mortar matrix, progressive activation of the FRP mesh, interaction with existing masonry joints, and possible contribution of connectors in limiting relative displacements. As a result, greater discrepancies arise when attempting to extrapolate formulations originally developed for thinner reinforcement systems. One of the most debated issues in the current literature concerns the explicit introduction, within capacity models, of a term accounting for the contribution of the added mortar layer. On the one hand, there is a clear rationale for considering the increase in wall thickness and the potential contribution of the mortar to shear resistance and stiffness. On the other hand, significant reservations remain regarding the appropriateness of including such a contribution in ultimate strength predictions for in-plane loaded masonry panels. Experimental observations indicate that mortar cracking may occur at drift levels substantially lower than those required to mobilize the ultimate tensile resistance of the embedded FRP grid within the CRM system, so purely additive formulations appear incorrect. Moreover, under cyclic loading, seismic actions, and post-fire conditions, this early cracking may reduce the effective contribution of the mortar, raising concerns that explicitly accounting for its strength contribution could lead to unconservative predictions of ultimate capacity. This issue warrants further research aimed at developing design formulations that provide conservative estimates while fully accounting for the beneficial contributions of all CRM composite components. Furthermore, deformation capacity and energy dissipation-related contributions of the strengthening systems, for which predictive models are currently lacking, need to be addressed to allow for more reliable nonlinear analyses.

10.3. Promoting knowledge transfer from academia to engineering practice

From a technology-transfer perspective, one of the main priorities for the scientific community is the development of design approaches that are structurally consistent with the format and reliability framework of the Eurocode. The transition from experimentally validated strengthening solutions to fully codified design procedures requires not only mechanical modelling advances, but also a systematic reliability-based calibration of capacity models. To this end, it is essential to analyse the available experimental databases at all relevant scales. This process should start from the mechanical characterisation of the constituent materials and extend to durability studies on CRM systems. At a higher structural level, the databases derived from tests on strengthened elements and subassemblies (e.g., panels under in-plane and out-of-plane loading, arches, and other structural components) should be assessed to probabilistically quantify the inherent variability of material properties, bond behaviour, cracking thresholds, and ultimate resistance parameters. This will make it possible to derive characteristic values, partial safety factors, and model uncertainty factors consistent with a semi-probabilistic limit state design approach, specifically tailored to CRM-strengthened masonry elements and suitable for practical design applications.

In this framework, advanced numerical modelling strategies may also play a key role in supporting the interpretation of experimental evidence and the development of mechanically consistent predictive models. These approaches could improve the understanding of the local interaction mechanisms between masonry substrate, mortar matrix, and CRM strengthening system, while also contributing to the calibration and validation of design-oriented formulations suitable for engineering practice and future code implementation. Lastly, no established guidelines currently exist for monitoring and controlling the performance of CRM interventions over time. This, together with the relatively young age of CRM systems and the still limited understanding of their long-term durability, highlights the need for further research to better evaluate the effectiveness of CRM strengthening in the long-term and the associated safety levels of reinforced structures along their expected lifespan.

CRediT authorship contribution statement

Stefano De Santis: Conceptualization, Data curation, Methodology, Supervision, Visualization, Writing – original draft, Writing – review & editing. **Maria Antonietta Aiello:** Project administration, Supervision. **Ingrid Boem:** Methodology, Visualization, Writing – original draft, Writing – review & editing. **Silvia Calò:** Data curation, Writing – original draft. **Alessio Cascardi:** Data curation, Methodology, Visualization, Writing – original draft, Writing – review & editing. **Tommaso D'Antino:** Validation. **Marielisa Di Leto:** Data curation, Visualization, Writing – original draft. **Natalino Gattesco:** Methodology. **Lidia La Mendola:** Supervision. **Francesco Micelli:** Methodology, Supervision, Writing – original draft. **Emanuele Rizzi:** Data curation. **Emanuela Speranzini:** Methodology.

Declaration of competing interest

The authors declare that there is no known competing financial interests or personal relationships that could have appeared to influence the work reported in this paper.

Acknowledgements

This work was carried out within the Research Project “DPC-RELUIS 2024-2026” funded by the Italian Department of Civil Protection, WP14 “Innovative Structural Materials for the Sustainability of Constructions”.

Data availability

Data will be made available on request.

References

[1] M.R. Valluzzi, M. Valdemarca, C. Modena, Behaviour of brick masonry vaults strengthened with FRP laminates, J. Compos. Construct. 5 (3) (2001) 163–169, https://doi.org/10.1061/1090-0268(2001)5:3(163).

[2] M.R. Valluzzi, D. Tinazzi, C. Modena, Shear behavior of masonry panels strengthened by FRP laminates, Constr. Build. Mater. 16 (7) (2002) 409–416, https://doi.org/10.1016/S0950-0618(02)00043-0.

[3] J.G. Tumialan, N. Galati, A. Nanni, Fiber-reinforced polymer strengthening of unreinforced masonry walls subject to out-of-plane loads, ACI Struct. J. 100 (3) (2003) 321–329, https://doi.org/10.14359/12607.

[4] G. Marcari, G. Manfredi, A. Prota, M. Pecce, In-plane shear performance of masonry panels strengthened with FRP, Compos. Struct. Part B Engineering 38 (7–8) (2007) 887–901, https://doi.org/10.1016/j.compositesb.2006.11.004.

[5] A. Borri, P. Casadei, G. Castori, J. Hammond, Strengthening of brick masonry arches with externally bonded steel reinforced composites, J. Compos. Construct. 13 (6) (2009) 468–475, https://doi.org/10.1061/(ASCE)CC.1943-5614.0000030.

[6] S. Babaeidarabad, A. Nanni, Plane Behavior of Unreinforced Masonry Walls Strengthened with fabric-reinforced Cementitious Matrix (FRCM), 299, ACI Special Publication, 2015, pp. 69–80.

[7] S.L. Sagar, V. Singhal, D.C. Rai, P. Gudur, Diagonal shear and out-of-plane flexural strength of fabric-reinforced cementitious matrix-strengthened masonry walletes, J. Compos. Construct. 21 (4) (2017) 04017016, https://doi.org/10.1061/CC.1943-5614.00007.
[8] G. Ramaglia, G.P. Lignola, A. Balsamo, A. Prota, G. Manfredi, Seismic strengthening of masonry vaults with abutments using textile reinforced mortar, J. Compos. Construct. 21 (2) (2017) 04016079, https://doi.org/10.1061/CC.1943-5614.0000733.
[9] S. Casacci, C. Gentilini, A. Di Tommaso, D.V. Oliveira, Shear strengthening of masonry wallettes resorting to structural repointing and FRCM composites, Constr. Build. Mater. 206 (2019) 19–34, https://doi.org/10.1016/j.conbuildmat.2019.02.044.
[10] C. D'Ambra, G.P. Lignola, A. Prota, F. Fabbrocino, E. Sacco, FRCM strengthening of clay brick walls for out of plane loads, Composites, Part B Eng. 174 (2019) 107050, https://doi.org/10.1016/j.compositesb.2019.107050.
[11] S. De Santis, F. Roscini, G. De Felice, Retrofitting of masonry vaults by basalt-textile reinforced mortar overlays, Int. J. Architect. Herit. 13 (7) (2019) 1061–1077, https://doi.org/10.1080/15583058.2019.1597947.
[12] R. Cucuzza, M. Domaneschi, G. Camata, G.C. Marano, A. Formisano, D. Brigante, FRCM retrofitting techniques for masonry walls: a literature review and some laboratory tests, Procedia Struct. Integr. 44 (2023) 2190–2197, https://doi.org/10.1016/j.prostr.2023.01.280.
[13] A. Cascardi, L.M. Koutas, S. De Santis, B. Ghiassi, F. Micelli, M.A. Aiello, T. Triantafillou, Textile-reinforced mortar (TRM) for retrofitting masonry structures: advantages, challenges and future potential, Mater. Struct. 59 (1) (2026) 38, https://doi.org/10.1617/s11527-025-02891-8.
[14] European Organization for Technical Approvals (EOTA), EAD 340392-00-0104. CRM (Composite Reinforced Mortar) Systems for Strengthening Concrete and Masonry Structures, 2020. Brussels, Belgium.
[15] Consiglio Superiore dei Lavori Pubblici (CSLLPP), Linea Guida per la Identificazione, la Qualificazione ed il Controllo di Accettazione dei Sistemi a Rete Preformata in Materiali Compositi Fibrorinforzati a Matrìce Polimerica da Utilizzarsi per il Consolidamento Strutturale di Costruzioni Esistenti con la Tecnica dell'Intonaco Armato CRM (Composite Reinforced Mortar). Rome, Italy, 2019 (in Italian).
[16] Consiglio Superiore dei Lavori Pubblici (CSLLPP), Circ 21/01/2019, n. 7. Istruzioni per l'applicazione dell'Aggiornamento delle Norme Tecniche per le Costruzioni di cui al DM 17/01/2018, GU 35 11/02/2019. Italian Building Code. (in Italian).
[17] Consiglio Nazionale delle Ricerche (CNR), Guide for the Design and Construction of Externally Bonded Fibre Reinforced Inorganic Matrix Systems for Strengthening Existing Structures. Rome, Italy, 2018. CNR-DT 215/2018.
[18] American Concrete Institute (ACI), Guide to Design and Construction of Externally Bonded Fabric-Reinforced Cementitious Matrix (FRCM) and Steel Reinforced Grout (SRG) Systems for Repair and Strengthening Masonry Structures. Farmington Hills, MI, USA, 2020. ACI 549.6R-20.
[19] C. Del Vecchio, M. Di Ludovico, A. Prota, Cost and effectiveness of fiber-reinforced polymer solutions for the large-scale mitigation of seismic risk in reinforced concrete buildings, Polymers 13 (2021) 2962, https://doi.org/10.3390/polym13172962.
[20] Regione Puglia. Prezzario Delle Opere Pubbliche - Edizione 2024. Bari, Italy. [In Italian].
[21] Consiglio Superiore dei Lavori Pubblici (CSLLPP), Linea Guida per la Identificazione, la Qualificazione ed il Controllo di Accettazione di Compositi Fibrorinforzati a Matrìce Polimerica (FRP) da Utilizzarsi per il Consolidamento Strutturale di Costruzioni Esistenti. Rome, Italy, 2019 (in Italian).
[22] European Organization for Technical Approvals (EOTA), Externally Bonded Composite Systems with Inorganic Matrix for Strengthening of Concrete and Masonry Structures. Brussels, Belgium, 2018. EAD 340275-00-0104.
[23] Consiglio Superiore dei Lavori Pubblici (CSLLPP), Linea Guida per la Identificazione, la Qualificazione ed il Controllo di Accettazione di Compositi Fibrorinforzati a Matrìce Inorganica (FRCM) da Utilizzarsi per il Consolidamento Strutturale di Costruzioni Esistenti. Rome, Italy, 2022 (in Italian).
[24] L. Righetti, M. Corradi, A. Borri, G. Castori, R. Sisti, A. Osofero, Durability of GFRP grids for masonry structures, Int. J. Forensic Eng. 3 (2016) 164–179, https://doi.org/10.1504/IJFE.2016.075990.
[25] N. Gattesco, I. Boem, Characterization tests of GFRM coating as a strengthening technique for masonry buildings, Compos. Struct. 165 (2017) 209–222, https://doi.org/10.1016/j.compstruct.2017.01.043.
[26] F. Micelli, M.A. Aiello, Residual tensile strength of dry and impregnated reinforcement fibres after exposure to alkaline environment, Compos. B Eng. 159 (2019) 490–501, https://doi.org/10.1016/j.compositesb.2017.03.005.
[27] S. De Santis, M.A. Caponero, S. Fares, C. Mazzotta, G. Moretti, An integrated system for structural strengthening and monitoring using CRM composites and FBG sensors, J. Build. Eng. 117 (2026) 114928, https://doi.org/10.1016/j.jobe.2025.114928.
[28] Consiglio Nazionale delle Ricerche (CNR), CNR-DT 200 R2/2025. Guidelines for the design, execution and inspection of structural strengthening interventions using fiber-reinforced composites. Materials, reinforced and prestressed concrete structures. Masonry Structures (Second Revision), 2025. Rome, Italy.
[29] Consiglio Nazionale delle Ricerche (CNR), CNR-DT 203 R1/2025. Guide for the Design and Construction of Concrete Structures Reinforced with Fiber-Reinforced Polymer Bars (First Revision). Rome, Italy, 2025.
[30] European Committee for Standardization (CEN), EN 1990:2002 Eurocode - Basis of Structural Design (Including Amendment A1:2005), 2002. Brussels, Belgium.
[31] V. Rizzo, A. Bonati, F. Micelli, M. Leone, M.A. Aiello, Influence of alkaline environments on the mechanical properties of FRCM/CRM and their materials, Key Eng. Mater. 817 (2019) 195–201, https://doi.org/10.4028/www.scientific.net/KEM.817.195.
[32] V. Fiore, T. Scalici, Bella G. Di, A. Valenza, A review on basalt fibre and its composites, Compos. B Eng. 74 (2015) 74–94, j.compositesb.2014.12.034.
[33] T. D'Antino, C. Papanicolaou, Mechanical characterization of textile reinforced inorganic matrix composites, Compos. B Eng. 27 (2017) 78–91, https://doi.org/10.1016/j.compositesb.2017.02.034.
[34] F. Micelli, A. Franco, R. Greppi, M.A. Aiello, Durability of CRM reinforcements. Life Cycle of Structures and Infrastructure Systems. Proceedings of the 8th International Symposium on Life Cycle Civil Engineering, IALCCE, 2023, pp. 2820–2827, https://doi.org/10.1201/9781003323020-343.
[35] O. Tamborrino, D. Perrone, M. Leone, M.A. Aiello, Experimental study on the fiber matrix interface behavior of FRCM/CRM reinforcement systems, Key Eng. Mater. 916 (2022) 409–416, https://doi.org/10.4028/p-0484vd.
[36] L.A. Bisby, V.K.R. Kodur, M.F. Green, Fire behavior of fiber reinforced cementitious composites, Fire Saf. J. 105 (2019) 1–14, https://doi.org/10.1016/j.apples.2021.100077.
[37] L. Estevan, B. Torres, F.B. Varona, F.J. Baeza, S. Ivorra, Shear strengthening of masonry walls with Textile Reinforced Mortars (TRM) under high temperature exposure, J. Build. Eng. 63 (2023) 105511, https://doi.org/10.1016/j.jobe.2022.105511.
[38] N. Gattesco, I. Boem, Experimental and analytical study to evaluate the effectiveness of an in-plane reinforcement for masonry walls using GFRP mesh, Constr. Build. Mater. 88 (2015) 94–104, https://doi.org/10.1016/j.conbuildmat.2015.04.014.
[39] A. Borri, G. Castori, M. Corradi, Design criteria for masonry reinforcement with Composite Reinforced Mortars (CRM), Key Eng. Mater. 916 (2022) 498–504, https://doi.org/10.4028/p-k031gd.
[40] Zoppo M. Del, M. Di Ludovico, A. Balsamo, A. Prota, In-plane shear capacity of tuff masonry walls with traditional and innovative Composite Reinforced Mortars (CRM), Constr. Build. Mater. 210 (2019) 289–300, https://doi.org/10.1016/j.conbuildmat.2019.03.133.
[41] American Society for Testing and Materials (ASTM) ASTM 519-07, Standard Test Methods for Diagonal Tension (Shear) in Masonry Assemblages. West Conshohocken, PA, USA, 2007.
[42] N. Gattesco, E. Rizzi, I. Boem, A. Dudine, M. Gams, A new method of seismic strengthening stone masonry with CRM coatings on one side, Constr. Build. Mater. 407 (2023) 133565, https://doi.org/10.1016/j.conbuildmat.2023.133565.
[43] N. Gattesco, I. Boem, E. Rizzi, A. Dudine, M. Gams, Cyclic tests on two-leaf rubble stone masonry spandrels strengthened with CRM coating on one or both sides, Eng. Struct. 296 (2023) 116965, https://doi.org/10.1016/j.engstruct.2023.116965.
[44] N. Gattesco, A. Dudine, Efficacia di una tecnica di rinforzo per murature con intonaco e rete in GFRP, in: Sicurezza e Conservazione nel Recupero dei Beni Culturali Colpiti dal Sisma, Venice, 8-9 April 2010 [In Italian].
[45] M. Corradi, A. Borri, G. Castori, R. Sisti, Shear strengthening of wall panels through jacketing with cement mortar reinforced by GFRP grids, Compos. B Eng. 64 (2014) 33–42, https://doi.org/10.1016/j.compositesb.2014.03.022.
[46] E. Mustafaraj, Y. Yardim, In-plane shear strengthening of unreinforced masonry walls using GFRP jacketing, Period. Polytech. Civ. Eng. 62 (2) (2018) 330–336, https://doi.org/10.3311/PPci.11311.

[47] N. Ismail, J.M. Ingham, In-plane and out-of-plane testing of unreinforced masonry walls strengthened using polymer textile reinforced mortar, Eng. Struct. 118 (2016) 167–177, https://doi.org/10.1016/j.engstruct.2016.03.057.

[48] N. Ismail, T. El-Maaddawy, A. Najmal, N. Khattak, Experimental in-plane performance of insulated concrete and brick masonry wall panels retrofitted using polymer composites, Bull. N. Z. Soc. Earthq. Eng. 51 (2) (2018) 85–91, https://doi.org/10.5459/bnzsee.51.2.85-91.

[49] M. Shabdin, M. Zargaran, N.K.A. Attari, Experimental diagonal tension (shear) test of Un-Reinforced Masonry (URM) walls strengthened with textile reinforced mortar (TRM), Constr. Build. Mater. 164 (2018) 704–715, https://doi.org/10.1016/j.conbuildmat.2017.12.234.

[50] T. D'Antino, F.G. Carozzi, C. Poggi, Diagonal shear behavior of historic walls strengthened with Composite Reinforced Mortar (CRM), Mater. Struct. 52 (2019) 114, https://doi.org/10.1617/s11527-019-1414-1.

[51] G. Guerrini, A. Bruggi, S. Urso, M. Quaini, A. Penna, Diagonal compression tests on stone masonry wallettes jacketed with different techniques, Key Eng. Mater. 916 (2022) 319–327, https://doi.org/10.4028/p-712sgu.

[52] M. Ponte, A. Penna, R. Bento, In-plane cyclic tests of strengthened rubble stone masonry, Mater. Struct. 56 (2023) 41, https://doi.org/10.1617/s11527-023-02126-8.

[53] C. Menna, D. Asprone, M. Durante, A. Zinno, A. Balsamo, A. Prota, Structural behaviour of masonry panels strengthened with an innovative hemp fibre composite grid, Constr. Build. Mater. 100 (2015) 111–121, https://doi.org/10.1016/j.conbuildmat.2015.09.051.

[54] A. Balsamo, D. Asprone, I. Iovinella, G. Maddaloni, C. Menna, A. Prota, F. Ceroni, A. Zinno, Effectiveness of inorganic matrix-grid composites for strengthening masonry walls. Proceedings of the 16th International Brick and Block Masonry Conference, June 2016, pp. 26–30. Padova, Italy.

[55] A. Borri, M. Corradi, R. Sisti, et al., Masonry wall panels retrofitted with thermal-insulating GFRP-reinforced jacketing, Mater. Struct. 49 (2016) 3957–3968, https://doi.org/10.1617/s11527-015-0766-4.

[56] F. Micelli, M.S. Sciolti, M. Leone, M.A. Aiello, A. Dudine, Shear behaviour of Fiber Reinforced Mortar strengthened masonry walls built with limestone blocks and hydraulic mortar. Proceedings of the 16th International Brick and Block Masonry Conference, Italy, Padova, June 2016, pp. 26–30, https://doi.org/10.1201/b21889-279.

[57] F. Longo, A. Cascardi, P. Lassandro, M.A. Aiello, Energy and seismic drawbacks of masonry: a unified retrofitting solution, J. Build. Pathol. Rehabil. 6 (1) (2021) 31, https://doi.org/10.1007/s41024-021-00145-2.

[58] A.R. Tilocca, A. Incerti, A. Bellini, M. Savoia, Influence of matrix properties on FRCM-CRM strengthening systems, Key Eng. Mater. 817 (2019) 478–485, https://doi.org/10.4028/www.scientific.net/KEM.817.478.

[59] P. Gulinelli, A. Aprile, R. Rizzoni, Y.H. Grunevald, F. Lebon, Multiscale numerical analysis of TRM-reinforced masonry under diagonal compression tests, Buildings 10 (2020) 196, https://doi.org/10.3390/buildings10110196.

[60] S. Calò, A. Cascardi, M.A. Aiello, Unified design-oriented model for the shear strengthening of masonry walls with Inorganic Mortar Composite systems, Eng. Struct. 336 (2025) 120394, https://doi.org/10.1016/j.engstruct.2025.120394.

[61] M. Betti, L. Galano, F.J. Pallarés, A numerical insight into the reliability of seismic strength models for masonry piers and spandrels, Eng. Fail. Anal. 152 (2023) 107430, https://doi.org/10.1016/j.engfailanal.2023.107430.

[62] P. Meriggi, S. De Santis, S. Fares, G. de Felice, Design of the shear strengthening of masonry walls with fabric reinforced cementitious matrix, Constr. Build. Mater. 279 (2021) 122452, https://doi.org/10.1016/j.conbuildmat.2021.122452.

[63] N. Gattesco, I. Boem, Influence of mortar coating type on the shear resistance of a GFRP based strengthening technique for brick masonry walls, in: Proceedings of the 16th International Brick and Block Masonry Conference, Padova, Italy, June 2016, pp. 26–30.

[64] A. Cascardi, F. Micelli, M.A. Aiello, Analytical model based on artificial neural network for masonry shear walls strengthened with FRM systems, Compos. B Eng. 95 (2016) 252–263, https://doi.org/10.1016/j.compositesb.2016.03.066.

[65] M. Angiolilli, A. Gregori, S. Cattari, Performance of Fiber Reinforced Mortar coating for irregular stone masonry: experimental and analytical investigations, Constr. Build. Mater. 294 (2021) 123508, https://doi.org/10.1016/j.conbuildmat.2021.123508.

[66] A.K. Thomoglou, T.C. Rousakis, D.V. Achillopoulou, A.I. Karabinis, Ultimate shear strength prediction model for unreinforced masonry retrofitted externally with textile reinforced mortar, Earthq. Struct. 19 (6) (2020) 411–425, https://doi.org/10.12989/eas.2020.19.6.411.

[67] F. Ferretti, C. Mazzotti, FRCM/SRG strengthened masonry in diagonal compression: experimental results and analytical approach proposal, Constr. Build. Mater. 283 (2021) 122766, https://doi.org/10.1016/j.conbuildmat.2021.122766.

[68] F. Longo, A. Cascardi, M.A. Aiello, In-plane strength of masonry panels reinforced with inorganic-based systems: novel design-oriented formulas, in: Construction Pathology, Rehabilitation Technology and Heritage Management - REHABEND, Granada, Spain, September 2022, pp. 13–16.

[69] K.E. Taylor, Summarizing multiple aspects of model performance in a single diagram, J. Geophys. Res. 106 (2001) 7183–7192.

[70] L. Sorrentino, D. D'Ayala, G. de Felice, M.C. Griffith, S. Lagomarsino, G. Magenes, Review of out-of-plane seismic assessment techniques applied to existing masonry buildings, Int. J. Architect. Herit. 11 (1) (2016) 2–21, https://doi.org/10.1080/15583058.2015.1011953.

[71] J. Donnini, G. Maracchini, S. Lenci, V. Corinaldesi, E. Quagliarini, TRM reinforced tuff and fired clay brick masonry: experimental and analytical investigation on their in-plane and out-of-plane behavior, Constr. Build. Mater. 272 (2021) 121643, https://doi.org/10.1016/j.conbuildmat.2020.121643.

[72] N. Gattesco, I. Boem, Out-of-plane behavior of reinforced masonry walls: experimental and numerical study, Compos. B Eng. 128 (2017) 39–52, https://doi.org/10.1016/j.compositesb.2017.07.006.

[73] N. Gattesco, E. Rizzi, I. Boem, A. Dudine, M. Gams, Seismic strengthening of existing brick masonry with CRM coatings on one side, Bull. Earthq. Eng. 23 (2025) 3779–3808, https://doi.org/10.1007/s10518-025-02181-2.

[74] A. D'Ambrisi, M. Mezzi, A. Caporale, Experimental investigation on polymeric net-RCM reinforced masonry panels, Compos. Struct. 105 (2013) 207–215, https://doi.org/10.1016/j.compstruct.2013.05.006.

[75] A. Bellini, A. Incerti, M. Bovo, C. Mazzotti, Effectiveness of FRCM reinforcement applied to masonry walls subject to axial force and out-of-plane loads evaluated by experimental and numerical studies, Int. J. Architect. Herit. 12 (2018) 376–394, https://doi.org/10.1080/15583058.2017.1412002.

[76] S. De Santis, G. De Canio, G. de Felice, P. Meriggi, I. Roselli, Out-of-plane seismic retrofitting of masonry walls with Textile Reinforced Mortar composites, Bull. Earthq. Eng. 17 (2019) 6265–6300, https://doi.org/10.1007/s10518-019-00702-5.

[77] S. De Santis, G. de Felice, Shake table tests on a tuff masonry structure strengthened with Composite Reinforced Mortar, Compos. Struct. 275 (2021) 114508, https://doi.org/10.1016/j.compstruct.2021.114508.

[78] P. Meriggi, G. de Felice, S. De Santis, Design of the out-of-plane strengthening of masonry walls with fabric reinforced cementitious matrix composites, Constr. Build. Mater. 240 (2020) 117946, https://doi.org/10.1016/j.conbuildmat.2019.117946.

[79] A. Borri, G. Castori, A. Grazini, Retrofitting of masonry building with reinforced masonry ring beam, Constr. Build. Mater. 23 (2009) 1892–1901, https://doi.org/10.1016/j.conbuildmat.2008.09.012.

[80] R. Sisti, M. Corradi, A. Borri, An experimental study on the influence of composite materials used to reinforce masonry ring beams, Constr. Build. Mater. 122 (2016) 231–241, https://doi.org/10.1016/j.conbuildmat.2016.06.120.

[81] I. Boem, N. Gattesco, E. Rizzi, A. Dudine, M. Gams, Fibre-based composite materials for the seismic strengthening of masonry ring beams: cyclic tests on full-scale samples, Mater. Struct. 58 (2025) 97, https://doi.org/10.1617/s11527-025-02617-w.

[82] N. Gattesco, I. Boem, V. Andretta, Experimental behaviour of non-structural masonry vaults reinforced through fiber-reinforced mortar coating and subjected to cyclic horizontal loads, Eng. Struct. 172 (2018) 419–431, https://doi.org/10.1016/j.engstruct.2018.05.009.

[83] A. Borri, P. Casadei, G. Castori, J. Hammond, Strengthening of brick masonry arches with externally bonded steel reinforced composites, J. Compos. Construct. 13 (6) (2009) 468–475, https://doi.org/10.1061/(ASCE)CC.1943-5614.0000027.

[84] V. Alecci, G. Misseri, L. Rovero, G. Stipo, M. De Stefano, L. Feo, et al., Experimental investigation on masonry arches strengthened with PBO-FRCM composite, Compos. B Eng. 100 (2016) 228–239, https://doi.org/10.1016/j.compositesb.2016.04.003.

[85] L. Garmendia, P. Larrinaga, R. San-Mateos, J.T. San-José, Strengthening masonry vaults with organic and inorganic composites: an experimental approach, Mater. Des. 85 (2015) 102–114, https://doi.org/10.1016/j.matdes.2015.06.013.

[86] S. De Santis, F. Roscini, G. de Felice, Full-scale tests on masonry vaults strengthened with steel reinforced grout, Compos. B Eng. 141 (2018) 20–36, https://doi.org/10.1016/j.compositesb.2017.12.023.
[87] F.G. Carozzi, C. Poggi, E. Bertolesi, G. Milani, Ancient masonry arches and vaults strengthened with TRM, SRG and FRP composites: experimental evaluation, Compos. Struct. 187 (2018) 466–480, https://doi.org/10.1016/j.compstruct.2017.12.053.
[88] T. Rotunno, M. Fagone, E. Grande, G. Milani, FRCM-to-masonry bonding behaviour in the case of curved surfaces: experimental investigation, Compos. Struct. 313 (2023) 116913, https://doi.org/10.1016/j.compstruct.2023.116913.
[89] S. De Santis, F. Roscini, G. de Felice, Retrofitting of masonry vaults by basalt-textile reinforced mortar overlays, Int. J. Architect. Herit. 13 (7) (2019) 1061–1077, https://doi.org/10.1080/15583058.2019.1597947.
[90] G. Ramaglia, G.P. Lignola, A. Balsamo, A. Prota, G. Manfredi, Seismic strengthening of masonry vaults with abutments using Textile Reinforced Mortar, J. Compos. Construct. 21 (2) (2017) 04016079, https://doi.org/10.1061/(ASCE)CC.1943-5614.0000713.
[91] N. Gattesco, I. Boem, A. Gubana, D. Menegon, N. Bello, A. Dudine, Experimental behavior of masonry vaults strengthened with thin extradosal or intradosal layer of fiber reinforced lime mortar, Key Eng. Mater. 747 (2017) 275–281, https://doi.org/10.4028/www.scientific.net/KEM.747.275.
[92] N. Gattesco, I. Boem, Review of experimental tests and numerical study on masonry vaults reinforced through fiber reinforced mortar coating, Bull. Earthq. Eng. 17 (2019) 4027–4048, https://doi.org/10.1007/s10518-019-00690-4.
[93] I. Boem, N. Gattesco, Cyclic behavior of masonry barrel vaults strengthened through Composite Reinforced Mortar, considering the role of the connection with the abutments, Eng. Struct. 228 (2021) 111518, https://doi.org/10.1016/j.engstruct.2020.111518.
[94] I. Boem, N. Gattesco, Composite Reinforced Mortar (CRM) and Fiber-Reinforced Cementitious Matrix (FRCM) for the seismic protection of masonry vaults, Procedia Struct. Integr. 44 (2023) 1260–1267, https://doi.org/10.1016/j.prostr.2023.06.160.
[95] A. Cascardi, S. Verre, F. Micelli, Strengthening of ceramic tubules-based vault: exploring CRM stiffening technique, in: IEEE International Conference on Metrology for Archaeology and Cultural Heritage, Valletta Campus, Malta, October .
[96] European Committee for Standardization (CEN), EN 1015-11 Methods of Test for Mortar for Masonry - Part 11: Determination of Flexural and Compressive Strength of Hardened Mortar, 2019. Brussels, Belgium.
[97] S. De Santis, O. AlShawa, G. de Felice, F. Gobbin, I. Roselli, M. Sangirardi, L. Sorrentino, D. Liberatore, Low-impact techniques for seismic strengthening fair faced masonry walls, Constr. Build. Mater. 307 (2021) 124962, https://doi.org/10.1016/j.conbuildmat.2021.124962.
[98] A. Borri, G. Castori, M. Corradi, R. Sisti, Masonry wall panels with GFRP and steel-cord strengthening subjected to cyclic shear: an experimental study, Constr. Build. Mater. 56 (2014) 63–73, https://doi.org/10.1016/j.conbuildmat.2014.01.056.
[99] M. Sangirardi, S. De Santis, I. Roselli, D. Liberatore, G. de Felice, A novel seismic-resistant reconstruction technique for fair-face rubblestone masonry, Eng. Struct. 334 (2025) 120210, https://doi.org/10.1016/j.engstruct.2025.120210.
[100] A. Artino, R. Caponetto, G. Evola, G. Margani, E.M. Marino, E. Murgano, Decision support system for the sustainable seismic and energy renovation of buildings: methodological layout, Sustainability 12 (24) (2020) 10273, https://doi.org/10.3390/su122410273.
[101] A. Artino, G. Evola, G. Margani, E.M. Marino, Seismic and energy retrofit of apartment buildings through autoclaved aerated concrete (AAC) blocks infill walls, Sustainability 11 (14) (2019) 3939, https://doi.org/10.3390/su11143939.
[102] F. Longo, A. Cascardi, P. Lassandro, A. Sannino, M.A. Aiello, Mechanical and thermal characterization of FRCM matrices, Key Eng. Mater. 817 (2019) 189–194.
[103] F. Longo, A. Cascardi, P. Lassandro, M.A. Aiello, A new Fabric Reinforced Geopolymer Mortar (FRGM) with mechanical and energy benefits, Fibers 8 (8) (2020) 49, https://doi.org/10.3390/fib8080049.
[104] F. Longo, A. Cascardi, P. Lassandro, M.A. Aiello, Thermal and seismic capacity improvements for masonry building heritage: a unified retrofitting system, Sustainability 13 (3) (2021) 1111, https://doi.org/10.3390/su13031111.
[105] J.P. Plassiard, M. Eymard, I. Alachek, O. Plé, Pushover tests on unreinforced masonry wallettes retrofitted with an innovative coating: experimental study and finite element modelling, Materials 14 (22) (2021) 6815.
[106] E. Parcesepe, R.F. De Masi, C. Lima, G.M. Mauro, M.R. Pecce, G. Maddaloni, Assessment of mechanical and thermal properties of hemp-lime mortar, Materials 14 (4) (2021) 882.
[107] A. Majumder, F. Stochino, F. Fraternali, E. Martinelli, Seismic and thermal retrofitting of masonry buildings with fiber reinforced composite systems: a state of the art review, Int. J. Struct. Glass Adv. Mater. Res. 5 (2021) 41–67.
[108] M. Mercuri, M. Vailati, A. Gregori, Two-heads brick masonry walls strengthened by basalt and glass chopped fiber mortar: effect of bed joints and coating reinforcements, Structures 64 (2024) 106530, https://doi.org/10.1016/j.istruc.2024.106530.
[109] L. Facconi, S.S. Lucchini, F. Minelli, G.A. Plizzari, Analytical model for the in-plane resistance of masonry walls retrofitted with steel fiber reinforced mortar coating, Eng. Struct. 275 (2023) 115232, https://doi.org/10.1016/j.engstruct.2022.115232.